EFFECTS OF CLIMATE CHANGE ON SLOPE STABILITY OF VARIABLY SATURATED EMBANKMENTS USING LOCAL FACTOR OF SAFETY AND IN-SITU STRESS FINITE ELEMENT ANALYSIS

Farsheed Bagheri

A THESIS SUBMITTED TO THE FACULTY OF GRADUATE STUDIES IN PARTIAL FULFILLMENT OF THE REQUIREMENTS FOR THE DEGREE OF

MASTER OF APPLIED SCIENCE

GRADUATE PROGRAM IN CIVIL ENGINEERING

YORK UNIVERSITY

TORONTO, ONTARIO

March 2022

Abstract

The global climate change process is actively underway and is expected to continue over the century. It has been predicted that the climate variables such as precipitation and potential evaporation will change significantly over the course of the century. Consequent changes in moisture content patterns within the earth structures, can destabilize, currently stable natural and engineered slopes and infrastructure embankments. A number of experimental and numerical studies have been conducted to study the effects of changing precipitation patterns and quantities on the stability of slopes. However, most of the previous researches used conventional limit equilibrium methods for slope stability assessment. In this research, extreme events impact on slope stabilities considering the initial moisture condition within the embankments is studied.

Moreover, the widely used conventional Limit Equilibrium (LE) methods for slope stability assessment are neither capable of analyzing the initiation of instabilities nor the process of potential surficial failures. These methods are also not capable of predicting shallow translational failure modes that have been observed for climate-induced slope instabilities. In this research, the effect of climate change on the stability of embankments is quantified by estimating a field of Local Factor of Safety (LFS) using a coupled in-situ stress finite element analysis and variably saturated flow analysis. In this method, the effect of moisture content variation on the effective stress is taken into account using suction stress state. Also, the initial moisture condition is considered based on statistical analysis of long-term variation of moisture content within the soil embankment using variably saturated flow analysis. The capability of the proposed simplified assessment approach in identifying global and local failure zones is compared to the elasto-plastic finite element analysis. As the case study, the effects of climate change on the stability of a typical highway embankment in Niagara Falls, London and Ottawa, in Ontario is studied.

Dedication

To the soul of my father Dr. Mohammad-Bagher Bagheri who taught me to never give up and to set the goals based on morality and rectitude. He was the greatest support and an inspiring role model for me and many others.

This thesis is dedicated to my beloved wife and children, Mina, Elena and Ryan Bagheri, who always stood by me. Without their love, support, and incredible understanding, I was not able to get here.

Acknowledgments

I wish to express my gratitude to my supervisor, Professor Rashid Bashir, for his support and help. He encouraged me to start this journey and to resume my academic learning several years after completion of my undergraduate degree. He helped me keep my hopes up particularly when the family and work responsibilities were at their peak in my life.

I would also like to thank Professor Lal Samarasekera for his patient support and constructive comments as the thesis committee member.

Special thanks to my adept colleague and friend, Dr. Ali Ghassemi whom I have had the honor of working with in the academia and industry. His contribution to this thesis was indeed remarkable.

Finally, and more importantly, I cannot thank my mother enough not only because of her exceptional support in all stages of my life, but also for her role as the origin of my success. She helped and encouraged me to build my career and education foundation in the old tough days of our lives.

Table of Contents

List of Tables

List of Figures

Chapter 1: Introduction

Climate change is a long-term shift in weather conditions primarily identified by changes in temperature and increase in the intensity and frequency of extreme weather events. Changes to the climate system are unequivocal and Canada is one of the countries that is warming at a faster rate than the world average (IPCC 2013). Climate warming will result in changes of other important climate variables, such as precipitation, and potential evaporation. Climate change involves both changes in average conditions and changes in variability, including frequency and intensity of extreme weather events. Strauch et al (2015) have indicated that climate change may cause the less frequent, but more intense rainfalls. According to IPCC (2013), it is expected that the frequency and intensity of the extreme precipitation events in North America will increase in the future. Pk (2017) investigated the changes in climate variables over the next 90 years in the City of Toronto. His research indicates that the mean annual temperature could potentially increase up to 6°C by the end of the 21st century. His research also shows that higher annual precipitation up to 18.5% can be expected with higher intensity extreme precipitation events.

Soil embankments are an important class of geotechnical infrastructure in transit and transportation networks. Due to permanent exposure to the environment, stability of embankments is highly dependent on the climate variables. Precipitation and evaporation are the two important climate variables that control the water balance at the embankment surface. The pore pressure distribution in the embankment is dependent on the water balance at the embankment surface. Increase in pore water pressure can reduce the shear strength of the unsaturated soil materials and can adversely affect the stability of embankments (Fredlund et

al. 2012). Shear strength is the amount of shear stress that soil can hold out against. The shear strength and how it can be mobilized is one of the important factors in slope stability.

Several researchers have used numerical modelling for the investigation of climate change impacts on the stability of slopes (e.g., Collison et al. 2000; Rouainia et al. 2009; Robinson et al. 2017; and, Pk et al. 2018). The majority of these slope stability assessment studies have been carried out using the widely used limit equilibrium method (LEM). However, the conventional limit equilibrium method is not generally capable of capturing local and shallow failures that are more likely to occur in slopes subjected to extreme precipitation events (Bagheri et al., 2019).

To accurately assess the behavior of embankments under changing climate, a deformation assessment using coupled hydro-mechanical analysis, with an appropriate elasto-plastic constitutive law may be required. This study is a part of an ongoing research about the effects of climate change on the stability of highway embankments across the province of Ontario. The objective of current study is to investigate the effect of climate change on the stability of soil embankments by estimating the field of Local Factor of Safety (LFS). In order to accomplish this objective, a coupled hydro-mechanical model using in-situ finite element analysis and unsaturated flow formulation, equipped with soil-atmosphere boundary condition was developed. The effect of water content variation on in situ effective stress field is taken into consideration using the suction stress state concept within the unsaturated soil mechanics framework. In this method, the in-situ stress field is calculated based on the elastic finite element analysis. The calculated LFS contour maps are compared to the yield zone obtained from an elasto-plastic finite element analysis. Moreover, conventional limit equilibrium method

and finite element-based limit equilibrium method in which the stability condition is identified in terms of single factor of safety were studied for the model verification purposes.

As a case study, the effects of climate change on the stability of a typical highway embankment consisting of sandy or silty soils in cities of Niagara Falls, London and Ottawa were assessed. The developed hydromechanical model was used to estimate the evolution of LFS field for 24 hours (6-hr historical and future design storms and 18-hr after the end of precipitation). The initial moisture condition within the embankments were obtained based on statistical analysis long term seepage analyses. In these analyses, the embankments were subjected to long-term historical and future climates for the locations under consideration.

1.1 Thesis Objective and Procedure

The objective of this research is to assess the capability of LFS method in analysis of slope instabilities under climate changes and study of the impact of different soil hydraulic parameters on embankment stability of typical highway soil embankments in three select cities in Ontario.

The numerical modeling and simulation of climate changes impact requires multiple hydrogeological, hydrological and geotechnical inputs. To achieve the above-mentioned preliminary approach, staged objectives were defined, and relevant studies were completed.

Figure 1.1 shows a summary of the implemented procedure and the objective of this research. In this research, a 30-year historical climate dataset (i.e., 1981-2010) and a 90-year (i.e., 2011-2100) future climate datasets were reviewed and introduced for the analysis. Assessment of local factor of safety and slope shallow failures during extreme precipitation events was carried out by introducing initial moisture content conditions based on statistical

analysis of long-term unsaturated flow analysis results for historical and future climate from the hydrological model into the finite element models in the form of coupled variably saturated flow and stress field analyses (i.e., Cube Module of HYDRUS 2D/3D program).

As illustrated below, the long-term climate data is introduced to the numerical HYDRUS 2D/3D model (soil-atmosphere model) and initial moisture condition of the slope interpreted accordingly. Moreover, extreme precipitation events extracted from the design intensity-duration-frequency (IDF) curves of climate data that relates duration, intensity of rainfall and frequency of occurrences to each other and can be used for forecasting of its hydrological and hydrogeological impact in future.

Both aforementioned initial moisture distribution and extreme precipitation events (extracted from the IDF curves) introduced to Cube Module of HYDRUS 2D/3D and the field of LFS assessed for the sandy and silty embankments in Niagara Falls, London and Ottawa.

Moreover, a LEM and an elasto-plastic constitutive law analysis carried out for one of embankments and the LFS results have been compared with LEM and elasto-plastic analysis. Assessment of the expected failure extent comparing the historical occurrences with the forecasted future impacts for both sandy and silty embankments have been presented as the conclusion of this research. Furthermore, based on the research conclusions, a guidance and proposed plan for future research has been compiled and presented.

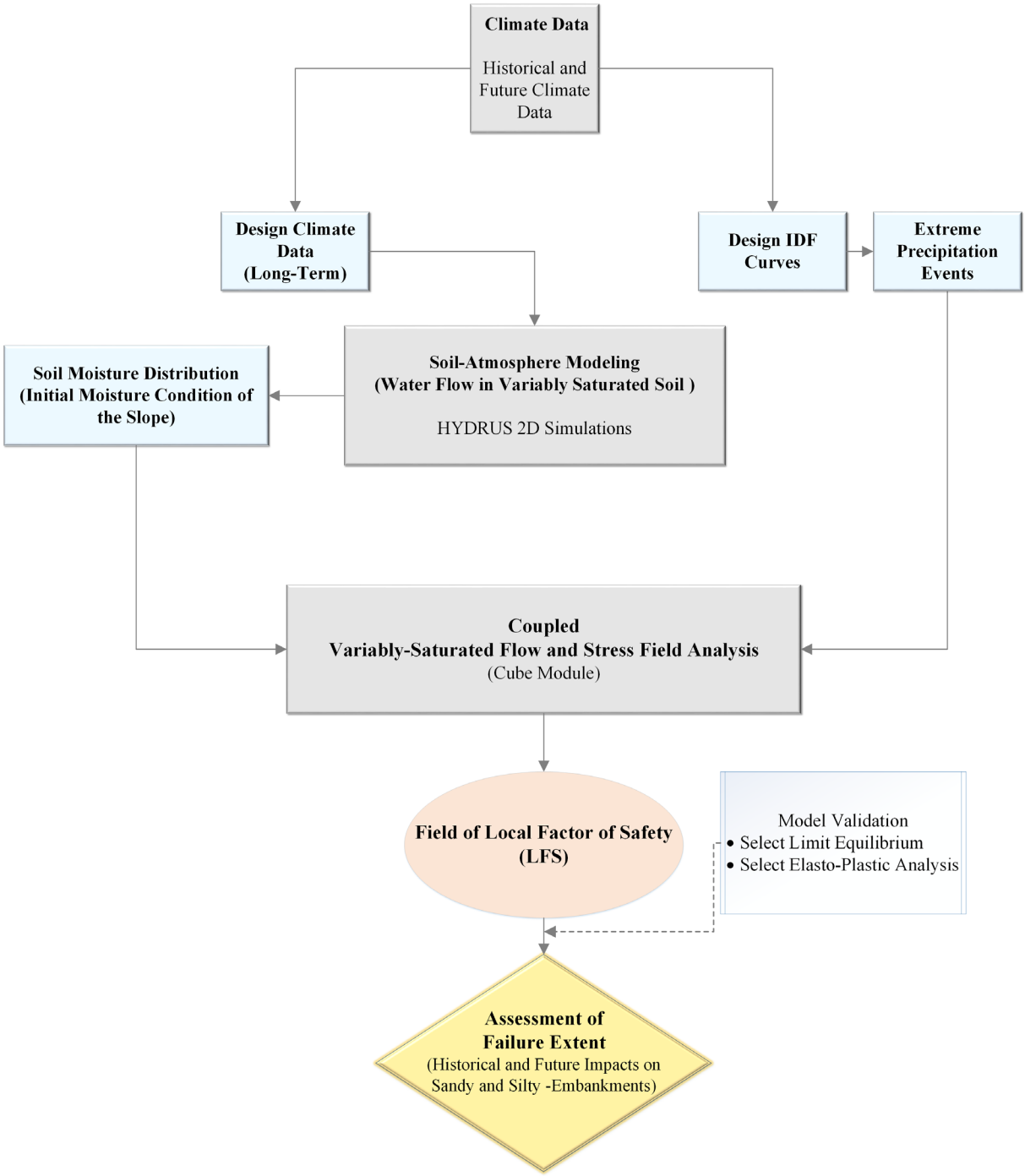

Figure 1.1 Research Procedure Flowchart

1.2 Thesis organization

This thesis has been organized into six (6) chapters:

- Chapter 1: presents the introduction of this research including objective and a summary of the procedures employed and accomplishments inline with planned objectives.
- Chapter 2: provides a review summary of technical background and the previous studies and their conclusions and limitations.
- The historical and future climate data, design climate including the extreme events and long-term design climate data analysis are discussed in the Chapter 3: this research.
- The Chapter 4: presents the carried-out research methodology including estimation of the field of local factor of safety (LFS) using suction stress, limit equilibrium method and elastic finite element modeling details. Moreover, the second part of this chapter presents the geometrical, geotechnical and hydrogeological details of typical MTO embankments in Ontario that have been simulated for this study in Niagara Falls, London and Ottawa in Ontario, Canada.
- In Chapter 5: findings, results, and discussions based on the research outcomes are presented. This includes an overview of results and comparison of the findings for highway embankments in the area of Niagara Falls, London and Ottawa.
- The conclusions of this research, a summary of findings and recommendations for future research are presented in Chapter 6: Moreover, the overview of the contribution of this research is presented in this chapter.
- References are presented at the end of this research.

- The Historical and Future IDF Curves for Niagara Falls, London and Ottawa are presented in Appendix A, and,
- Evolution of Area of LFS <1 (m^2) vs Precipitation time (6 hours) and assessment time (24 hours) for Embankments in London and Ottawa are presented in Appendix B.

Chapter 2: Theoretical Background

2.1 Climate Change

The human influence on changing climate is obvious and greenhouse gases are at the highest amount in the atmosphere impacting natural systems and humans (IPCC 2014). These impacts will be irreversible and will cause long-lasting changes in climate. The climate change impact and potential risks associated with it will not be evenly distributed across the globe. According to IPCC 2014, there are likely more regions across the globe experiencing more frequent and intense precipitation and, north America is one of them which likely will experience higher frequency and intensity of heavy precipitation events. Based on IPCC 2014, climate change is a threat to sustainable development and adaptation and mitigation measures are suggested. In urban areas, impact of climate changes, particularly storms and extreme precipitation will likely amplify the relevant damaging risks for lacking essential infrastructures and assets.

Fallah-Ghalhari et al. (2019) studied the impacts of climate changes on maximum and minimum temperatures. They indicated that the identification of the behavior of extreme weather events is a key factor in climate change globally. They referred to the studies that have shown that the change in the frequency and intensity of extreme events relative to the change in mean climatic parameters will possibly have more notable adverse impact on different aspects of human society and infrastructure (Brown 2004,

Tao et al. 2012, and, Labajo et al. 2014). They indicated that the important impacts due to the climate changes are extreme events related to temperature and precipitation. They concluded that people should be prepared to overcome these extreme events that may produce short-term and long-term effects affect on human health, community, and infrastructures (López-Diaz et al. 2013, Kwak et al. 2015, and, Scripca et al. 2016).

Vincent et al. (2018) studied the changes in Canada's climate and declared the Canada's climate is changing. They reviewed the data from all stations in Canada for the period of 1948 to 2016 and southern Canada stations' data for the period of 1900 to 2016. Their study was carried out based on daily temperature and precipitation data. They concluded that in southerly regions of Canada the number of hot days and hot nights have increased. In general, frost-free seasons are longer and the climate changes trend is inline with warming and larger trends observed related with cold temperatures in winter. They indicated that number of rainy days with heavy precipitation is increased. According to their study, although there is no consistent trend for extreme precipitation, total increase in precipitation have been noted. Southern British Colombia (BC) and Ontario found with more wet days due to climate change. Moreover, very wet days have increased in BC, southern Quebec and southern Ontario. Vincent et al. (2018) also concluded that the climate change can have an adverse impact on road maintenance (Schmidlin et al., 1987, Hershfield, 1979, and, Ho & Gough, 2006).

Pk (2017) assessed the variation of Toronto, Ontario climate parameters for the next 90 years. He concluded that the quantity and intensity of precipitation in the future may possibly become approximately 100% greater than the historical period. He reported that the yearly increase in trend of precipitation amount and extreme events are expected in the future.

Taban et al. (2019) published the Chapter 4 of Canada's Changing Climate Report (CCCR), assessing observed (historical) and projected (future) changes in temperature and precipitation across Canada. They reported with "medium confidence" that the yearly average precipitation in Canada has increased and it is "virtually certain" that Canada's climate will be warmer in future as it already warmed. It is noteworthy, that CCCR has indicated that with "high confidence" daily extreme precipitation event will increase. They reported that increase in precipitation can cause

damages to the roads and their infrastructures. Similar to Vincent et al (2018) assessment, CCCR reported that several locations across Canada including southern Ontario is expected to experience more frequent extreme precipitation events and longer duration extreme event may cause more significant damages and flooding.

2.2 Slope Stability under Changing Climate

Numerical simulation of climate change impact on slope stability requires a multi-disciplinary approach. This includes a climate model to provide high-resolution future climate dataset as well as a hydrological model to simulate variably saturated flow due to soil-atmosphere interaction. Further, a proper geotechnical model is required for slope stability assessment considering the effects of suction on shear strength of the soil. Several researchers have proposed numerical models for investigation of climate change impacts on the stability of slopes (e.g., Collison et al. 2000; Rouainia et al. 2009; Robinson et al. 2017; Pk et al. 2018). Even though the soil-atmosphere interaction (precipitation and evaporation) is more likely to cause shallow and local failures, most of the previous studies have only considered the general or deep-seated failures using the conventional limit equilibrium methods.

Changes in extreme precipitation patterns due to climate change have the potential to affect the stability of both natural and constructed slopes. Highway embankments are continuously exposed to changing climate conditions and water exchanges takes place at the soil-atmosphere boundary of slopes. It will change the water storage in the slopes that would cause an increase in the pore water pressure and a decrease in the suction stress and subsequently the soil shear strength. These changes in pore pressure and shear strength can lead to slope instabilities Fredlund et al.

(2012). However, it is complex to predict the changes in climate and determine their related impact on the geohydrological hazards, including landslides (Gariano & Guzzetti, 2016).

Several researchers have proposed numerical models for investigation of climate change impacts on the stability of slopes (e.g., Collison et al. 2000; Rouainia et al. 2009, Robinson et al. 2017, Pk et al. 2018, Baninajarian 2020). The majority of slope stability assessment studies have been carried out using the widely used limit equilibrium method (LEM). However, the conventional limit equilibrium method is not generally capable of capturing local and shallow failures that are more likely to occur in slopes subjected to extreme precipitations (Bagheri et al., 2019 and 2020).

Dikau & Schrott (1999) carried out a European project titled "The temporal stability and activity of landslides in Europe concerning the climatic change (TESLEC)," to assess the relationship between landslides and climate over time. They studied eight sites located in five different European countries (i.e., England, France, Italy, Portugal, and Spain). The main factor for the selection of these locations was landslide data and recent studies. They concluded that a single "universal law" for all of Europe is not feasible because the relationships between climate and landslides are different and complex.

Collison et al., (2000) assessed the potential impact of predicted climate change on landslides in southeast England. They modelled a 4 km section of a slope using a hydro-geotechnical simulation and global climate model (GCM) inputs on a geographical information system (GIS) model. Their results demonstrated that climate change would not cause frequent massive landslides; however, water content and storage in shallow depths could potentially increase, which may change the frequency and periods of instability.

Schmidt & Dikau, (2004) studied the effect of historical climate variability on slope stability. They assessed the stability of hillslopes under changing climate at three hillslopes near Bonn (Germany). Their results showed that the stability of landslides is sensitive to climatic changes. They found out that sensitivity to climate change is dependent on the geometry, location of sensitive layers, and the soil types. They also found that the modelled climate scenario with a higher frequency of intense rainfall events were generally more detrimental to slope stability.

Dixon & Brook (2007) assessed the potential effect of global climate change on the active Mam Tor landslide in the UK. They used historical climate data obtained from a weather station that was located approximately 10 km southwest of Mam Tor. Future precipitation predicted from the UKCIP 2002 report based on a future climate change model (HadCM3). They indicated that Mam Tor could be more vulnerable to the predicted precipitation and could experience rapid slope instability due to the wetter conditions. This was due to expected more frequent rainfall.

Rahardjo et al. (2010) investigated the effects of the position of the groundwater table, rainfall intensity, and soil properties on the stability of different natural slopes in Singapore. They considered three different groundwater table positions, corresponding to the normal, dry, and wet scenarios. They also considered four different precipitation intensities of 9, 22, 36, and 80 mm/h. The two main residual soils in the study area, were Bukit Timah Granite and the Sedimentary Jurong Formation. They reported that the position of the groundwater table during rainfall did not significantly affect the factor of safety. This was due to relatively small changes in the matric suction. They also reported that soil properties had a large effect on the factor of safety. A higher percentage of fine particles in the soil leading to higher air-entry value and lower soil permeability, reduces the factor of safety rapidly during the precipitation events. They also noted that the minimum factor of safety might occur even several hours after the end of the precipitation event.

This would be due to the deeper and progressive infiltration and percolation of precipitation to the critical slip surface depth hours after the end of the rainfall. They also mentioned that slope geometries and soil properties have a notable relation with the slope general factor of safety.

Coe & Godt (2012) identified fourteen technical approaches for assessing the impact of climate change on landslide activity. They classified these approaches as 1) long-term monitoring of climate change and landslide activities, 2) establish a connection between climate data and landslide activity based on historical records, and 3) develop patterns between historical landslide activity and climate records. They then used these approaches with future climate predictions to assess expected upcoming landslide activity. They concluded that predicting the frequency and intensity of future extreme events are a complex subject that leads to some uncertainties in assessment of shallow landslides.

Rianna et al. (2014) investigated the long-term behaviour of Orvieto clayey landslide in Italy. They used a 30-year-long monitoring record of the landslide and established a relationship between rainfall and rate of landslide movement. They used historical climate data for future climate prediction they used COSMO-CLM data (Rockel and Geyer, 2008) based on two different emission scenarios (i.e., RCP4.5 and RCP8.5). They predicted the slope displacement until the end of 2100 and concluded that the predicted climate changes could potentially cause a significant landslide movement and instability.

Ciabatta et al., (2016) assessed the impact of climate-change scenarios on landslide in the Umbria Region, Italy. They downscaled the outputs of five different GCMs and applied weather generators to convert daily rainfall and temperature data to hourly data. Then, they estimated the number of landslide occurrence for three distinct periods, 1990–2013 (as the baseline), 2040–2069 and 2070–2099. They concluded that the number of landslides could increase by up to 45% in the

future. They also observed that there is not a simple relation between climate parameters and the number of landslides, and suggested importance of soil moisture conditions should be considered. They concluded that during the wet season, the number of landslide events would increase significantly because of the increase in soil moisture content. They also mentioned that the type of GCM scenarios and climate data resolution could influence the results.

Batali & Andreea (2016) investigated the slope stability taking into consideration the unsaturated soil conditions. They investigated the slope stability of a landslide located in Cluj-Napoca city, in Romania considering various unsaturated shear strength values predicted by different models. They also assessed the importance and impact of a drainage system on the slope stability of their case study. They noted that the models based on Fredlund and Xing (1994) unsaturated soil parameters show acceptable performance in the model in comparison with the in-situ results and measured values of suction. They concluded that more realistic results could be obtained if unsaturated properties are considered in the slope stability assessment process. They also reported an increase in values of factor of safety for consideration of unsaturated soil properties. Improvement in slope stability due to the drainage system was also reported.

Robinson et al. (2017) assessed the effect of extreme rainfall events on a homogeneous silty soil slope under current and future climate scenarios. They selected Seattle, Washington, as the study area using the historical and future intensity-duration-frequency (IDF) curves. They obtained the future precipitation data from a coupled model project called Coupled Model Intercomparison Project Phase 5 (CMIP5) (Taylor, 2012). They used a fully coupled two-dimensional stress-strain and unsaturated flow finite element model. The model considered a 7-day duration of baseline and future rainfall data as the initial condition. Their results indicate that the increase in future rainfall

intensity could result in increasing the pore water pressure that would negatively affect the stability of the embankment slope by changing the suction stress.

Pk et al. (2018) studied the effect of climate change on the stability of embankments. They quantified the effects of future long term and extreme precipitation events on the probable instability of a typical sandy and silty highway embankments in southern Ontario, Canada. For their analysis, they used a two-dimensional (2D) transient variably saturated seepage finite-element model to analyze pore-water pressures and a 2D limit equilibrium slope stability model for stability assessments. Their results indicated that the future infiltration could increase by 41%, which would result in a 30% reduction in the embankments' factor of safety. They also reported that the hydraulic properties of variably saturated soils would have a significant impact on the embankment's stability under changing climate. They concluded that, silty embankments with low permeability have a lower factor of safety (FOS) as finer materials retain water more and conduct the water gradually.

One can see the importance of the impact of climate changes on infrastructure such as embankments and slopes has been emphasised by several researches. It has been repeatedly reported that intensity and frequency of future extreme events will have an important impact on human life and infrastructures. This complex issue, that is now a known problem, needs more assessment and scientific studies.

2.3 Unsaturated Soil Mechanics Framework

Matric suction or negative pore pressure has the effect of increasing the shear strength of unsaturated soils. Therefore, considering the contribution of matric suction in the slope stability assessment is of great importance (Fredlund et al. 2012; Adem, H. and Vanapalli 2014, and, Arairo

et al. 2015). Unsaturated shear strength can be considered as a function of the two stress variables i.e., net normal stress and matric suction. The most frequently used two stress state variables method has been proposed by Vanapalli et al. (1996) as follows:

$$\tau = c' + (\sigma - u_a)\tan\phi' + (u_a - u_w)[(S_e)\tan\phi'] \quad \text{Equation 2.1}$$

Where c' is effective cohesion intercept, u_a is pore-air pressure, u_w is pore water pressure, (σ - u_a) is net normal stress on the failure plane, (u_a - u_w) is matric suction, ϕ' is effective angle of internal friction for the saturated soil, and S_e is the effective degree of saturation as described below:

$$S_e = \frac{\theta - \theta r}{\theta s - \theta r} \quad \text{Equation 2.2}$$

Lu and Likos, (2006) extended the pioneer work by Bishop, to define a new stress variable called suction stress (σ^s) in the Terzaghi's effective stress equation:

$$\sigma' = (\sigma - u_a) - \sigma^s \quad \text{Equation 2.3}$$

The suction stress defined as a function of matric suction by developing suction stress characteristic curve (SSCC). Later, Lu et al., (2010) proposed a closed-form expression for suction stress for the full range of matric suction:

$$\sigma^s = -(u_a - u_w) \qquad u_a - u_w \leq 0 \qquad \text{Equation 2.4}$$

$$\sigma^s = \frac{(u_a - u_w)}{(1+[\alpha(u_a - u_w)]^n)^{(n-1)/n}} \qquad u_a - u_w > 0 \qquad \text{Equation 2.5}$$

where α and n are the empirical parameters as defined in the soil water characteristic curve (SWCC) function by van Genuchten's (1980) model. Similarly, an expression for suction stress in terms of effective saturation can be written as follows (Lu et al., 2010):

$$\sigma^s = -\frac{S_e}{\alpha}\left(S_e^{\frac{n}{1-n}} - 1\right)^{\frac{1}{n}} \qquad 0 \leq S_e \leq 1 \qquad \text{Equation 2.6}$$

In this study, the single stress state approach by Lu et al. was used to develop hydro-mechanical models to assess the stability of slopes using effective stress field in variably saturated embankments subjected to soil-atmosphere interaction. The effective stress field is the basis for developing LFS contours, as described in Section 2.4.

2.4 Local Factor of Safety (LFS)

The most widely used analytical technique to carry out slope stability analyses is the limit-equilibrium method (LEM) of slices (Fellenius, 1936, Janbu, 1973, Duncan, and, Wright, 2003). Shear strength reduction method is also a common slope stability method used in geotechnical engineering (Smith and Griffiths, 2004). In 2012, Lu et al. introduced a stress field-based method that defines the factor of safety at each point in a slope. Assessment of the factor of safety at each point is different from conventional single factor of safety that limit-equilibrium based methods present. A framework in the form of Slope Cube module added in the Hydrus 2D/3D (Šimŭnek et

al., 2008) by Liu and Godt in 2013. Slope Cube can simulate and assess the expected timing and location of failure initiation in variably saturated slopes (Lu et al. 2016).

Each point within a slope is assessed by calculating the ratio of the existing Coulomb stress at the studied point to the Coulomb stress of the potential failure state based on the Mohr-Coulomb principal of classic soil mechanics and the result presented as the Local Factor of safety. This method first quantifies the field of FS based on the concept of the Coulomb stress and then by calculating the state of stress changes toward failure due to the precipitation into the variably saturated zone of slopes and embankments.

Lu et al., (2012) mentioned that limit-equilibrium methods are commonly used by geotechnical engineers due to their established "effectiveness and reliability". They concluded limit equilibrium method provides only approximate location and geometry of the potential failure surface.More importantly, it was clarified that the LEM do not provide sufficient insight into the location of initial failure or progress of failure due to changes in the pore water pressure. Moreover, they introduced and described an approach that calculates a scalar field of FS to address the limitations of conventional FOS methods for flow and stress field assessments in variably saturated zone of slopes.

Lu et al., (2012) defined the local factor of safety (LFS) as the ratio of Coulomb stress of the potential failure state under the Mohr-Coulomb criterion (τ^*) to the Coulomb stress at the current state of stress (τ) (Equation 2.7).

$$LFS = \frac{\tau^*}{\tau} \qquad \text{Equation 2.7}$$

Figure 2.1 illustrates the definition of τ^* and τ for a given Mohr circle stress state on a shear stress-normal stress space. As can be seen on this figure, while the state of stress in a slope represented by the Mohr circle is below the Mohr-Coulomb failure envelope, the LFS is greater than unity. LFS can also be easily derived based on the mean and deviator effective stresses (p' and q') in two-dimensional space as follows (Lu et al., 2012):

$$LFS = \frac{2\,cos\emptyset'}{q'}\,(c' + p'\tan\emptyset') \qquad \text{Equation 2.8}$$

where c′ is the drained cohesion of the slope material, $\emptyset'$ is the drained friction angle of the material. LFS can be calculated at each point using Equation 2.8. A LFS contour map can be obtained by joining the points with same LFS values indicating stability condition of an earth slope. The zones with LFS greater than unity imply statically stable conditions, while zones with LFS equal or less than unity, are at the limit state and local failure can be expected.

It should be noted that soil-atmosphere interaction (precipitation and evaporation) affects the pore water pressure (PWP) distribution through embankment fill over time. This leads to the evolution of the effective stress fields that consequently affects the LFS field. The changes in effective stress field can be estimated by calculating the suction stress based on single stress state variable framework of Lu and Likos (2006) as described earlier in this chapter.

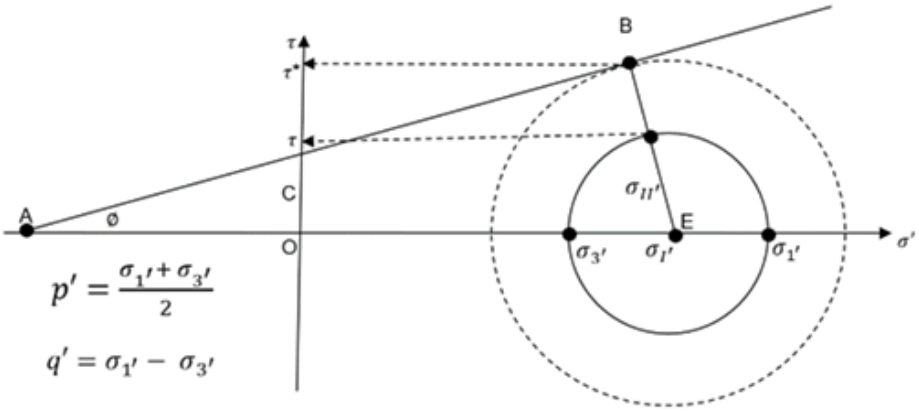

Figure 2.1 Illustration of definition of τ^* and τ for a given Mohr circle stress state (Adopted from Lu et al., 2012)

The LE method is known to be an effective and reliable method of slope stability analysis. Although theoretically there is no limitation on depth of failure in LEM, it is a common practice to specify a minimum sliding mass depth in limit equilibrium analyses to not consider shallow slip surfaces. This minimum slip depth is usually defined around 1.0 to 1.5 m. Failures shallower than such assumptions are generally considered too shallow that would affect operation and maintenance procedures. In addition, LEM typically seeks a single stability indicator for the entire slope. Thus, even considering lower value for minimum sliding mass depth, LEM cannot provide local failure zones that might be the location of initial future global failures (Lu et al., 2012). Therefore, one can see the importance of employing LFS method for slope stability analysis that can assess the impact of precipitation on embankment stability especially the shallow initial failures.

Yeh and Tsai (2018) analyzed the effect of soil hydraulic conductivity anisotropy on slope stability using a coupled hydromechanical framework. They investigated the effect of rainfall and transient seepage on stability of the top of the slope, along the slope and at the toe of the slope.

They concluded that rainfall infiltration and slope safety can be assessed using a coupled hydromechanical framework. They declared that their study shows advantages of LFS method because the impact of rainfall on slope stability variation at each point was evaluated "with space and time". Moreover, it was concluded that limit equilibrium methods (e.g., Bishop's simplified method, the Morgenstern and Price method, etc.) can be used to easily calculate the safety factor of a slope by assuming failure surface, whereas to identify location the slope failure initiation and the real failure surface LFS method is the appropriate approach of slope stability analysis.

In conclusion, one can see the relatively new LFS method has many advantages over conventional slope stability analysis methods including but not limited to identifying the initial pattern of a slope failure, accurate slip and failure surface and recognizing the impact of precipitation on slope stability.

Chapter 3: Climate Data and Design Storms

3.1 Introduction

The highway embankments are exposed to the atmospheric conditions and are influenced by the changing climate conditions. Process of water exchange across the soil-atmospheric boundary of embankments results in changes in the embankment water storage. The suction element of soil shear strength decreases when the pore water pressure increases within the unsaturated (vadose) zone of embankments and can potentially cause slope instabilities (Fredlund et al. 2012). In addition to the geometry of soil embankment slope, the slope stabilities are dependant on the soil unit weight, hydraulic parameters, and shear strength parameters, and the incipient moisture condition of the embankment at the start of an extreme precipitation event. As can be seen on Figure 3.1, embankment slopes are exposed to the atmosphere and the water exchange occurs through the soil-atmospheric boundary.

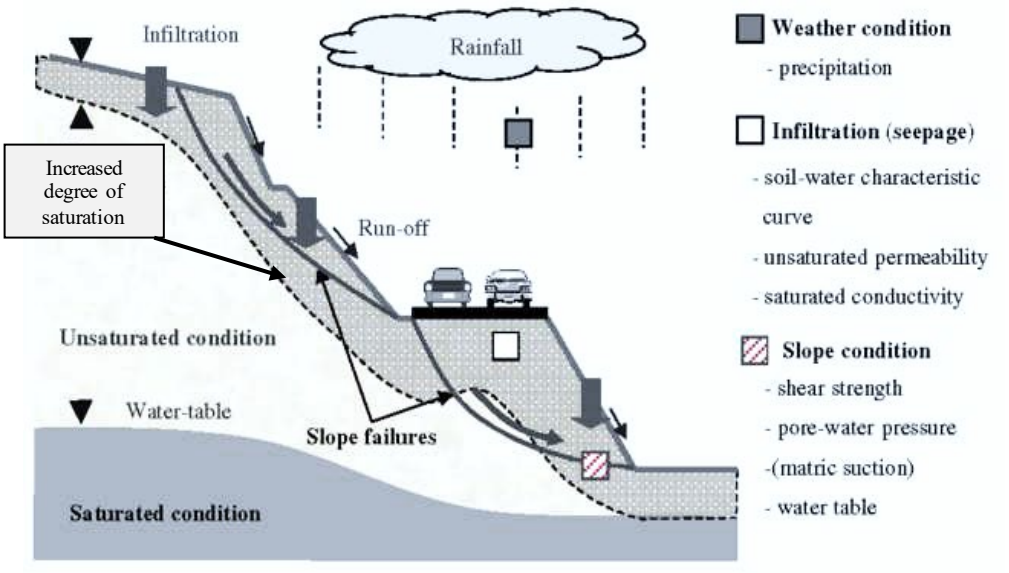

Figure 3.1 Embankment Soil-Atmospheric Interaction (modified from Lee et al., 2009)

In this chapter, procedure used in this study for the selection of climate data is presented. This includes the use of historical and future climate data for three different locations across southern Ontario. The short-term climate data (i.e., extreme events) and long-term design climates for slope stability assessments carried out by Baninajarian (2020) and Bashir et al. (2021) are reviewed and appropriate selection of data for this research is presented in this chapter. Extreme precipitation introduces significant amount of water to the embankments that have already contained some moisture content due to expected long-term climate condition. To assess the soil embankment stability under the extreme precipitation effects, appropriate existing moisture content (i.e., initial moisture content) using the long-term climate data was considered in this research.

3.2 Climate Data

In general, the climate data used in this research is compiled from the research carried out by Baninajarian (2020) and Bashir et al. (2021). From their studies, the long-term and extreme precipitation climate data for the cities of Niagara Falls, London and Ottawa was extracted, analyzed and used in the analysis of slope stability assessments.

3.2.1 Historical and Future Long-Term Climate Data

Historical climate data (baseline climate) is used to assess the probable changes in the future climate. This data was collected from the Environment and Climate Change Canada data portal (Environment and Climate Change Canada 2018). This dataset comprised of the daily values of precipitation, maximum and minimum temperature, and relative humidity, windspeed

and net radiation values for ten different locations across Ontario. The dataset covers a period of 30 years spanning from 1980-2010. Other pertinent details of this dataset such as the relevant weather stations can be found in Bashir et al. (2021) report.

Future climate data obtained from Ontario Climate Change Data Portal (OCDP) published by the Laboratory of Mathematical Parallel System (LAMPS) at York University (https://lamps.math.yorku.ca/OntarioClimate/index.htm). Pk et al. (2018) and Bashir et al. (2021) and have indicated that the modeling done by OCDP predicts the historical climate data better than similar attempts by others, i.e., Canada Climate Change Data Portal (CCDP), 2018. Therefore, climate data from Ontario Climate Data Portal (OCDP) was used in current research. The OCDP dataset spans a period from 1980 to 2100. It is understood that OCDP dataset contains four climate variables, i.e., daily values of precipitation and minimum, maximum, and average temperatures. This data is available for a 10×10 km grid across Ontario. This data is available for many GCMs and all four representative concentration pathways (RCPs), i.e., RCPs 2.6, 4.5, 6.0, and 8.5. Previous studies by Pk et al. (2018) and Bashir et al., (2020) have indicated that among all the GCMs, CCSM4, GFDL-ESM2M, Had GEM2_ES, and NorESM1-M show better performance in predicting the historical data. Therefore, data for these four GCMs for all four RCPs were used in this research.

The climate data from four above mentioned GCM and all four RCPs, resulted in 48 case studies of thirty-year climate datasets for each of the cities under consideration (Baninajarian , 2020). Each climate dataset corresponds to a particular GCM, RCP and one of three future time periods, representing the start, middle and end of the century (2011-2040, 2041-2070, 2071-2100). Baninajarian (2020) carried out a detailed assessment of the whole dataset using the soil-atmosphere modeling to identify the dataset which could potentially produce most detrimental

conditions in terms of the stability of the slopes. The details of this assessment can be found in Baninajarian (2020). Table 3.1 presents the details of the identified detests for the cities of Ottawa, London, and Niagara Falls.

Table 3.1 Identified datasets for the regions under consideration

City	GCM	RCP	Time Period
Niagara Falls	GEM2-ES	2.6	2011-2040
London	GFDL-ESM2M	6.0	2011-2040
Ottawa	GEM2-ES	2.6	2011-2040

3.2.2 Climate Classification

Climate classification provides a general view and guidance about water availability and weather setting that can be very useful for a geotechnical engineer for a particular site. The Thornthwaite climate classification system (Thornthwaite, 1948, Thornthwaite & Hare, 1955) is an empirical method of climate classification used for engineering purposes. The system was developed from climatic data collected in the United States based on the calculation of the annual moisture index and requires estimates of annual precipitation and potential evaporation. The annual moisture index is defined as follows (Thornthwaite & Hare, 1955):

$$I_m = 100\left(\frac{P}{PE} - 1\right) \qquad \text{Equation 3.1}$$

where I_m is the annual moisture index, P is the total annual precipitation, and PE is the total annual potential evaporation.

Equal values of annual precipitation (P) and the potential evaporation (PE) result in I_m value of zero, which signifies net neutral water availability conditions at the ground surface. A positive I_m value implies a surplus of the water availability, and the climate conditions could range from moist humid to perhumid. While a negative I_m value indicates a scarcity of the water availability, and the climatic conditions could be from dry subhumid to arid. The annual moisture index (I_m) is shown on

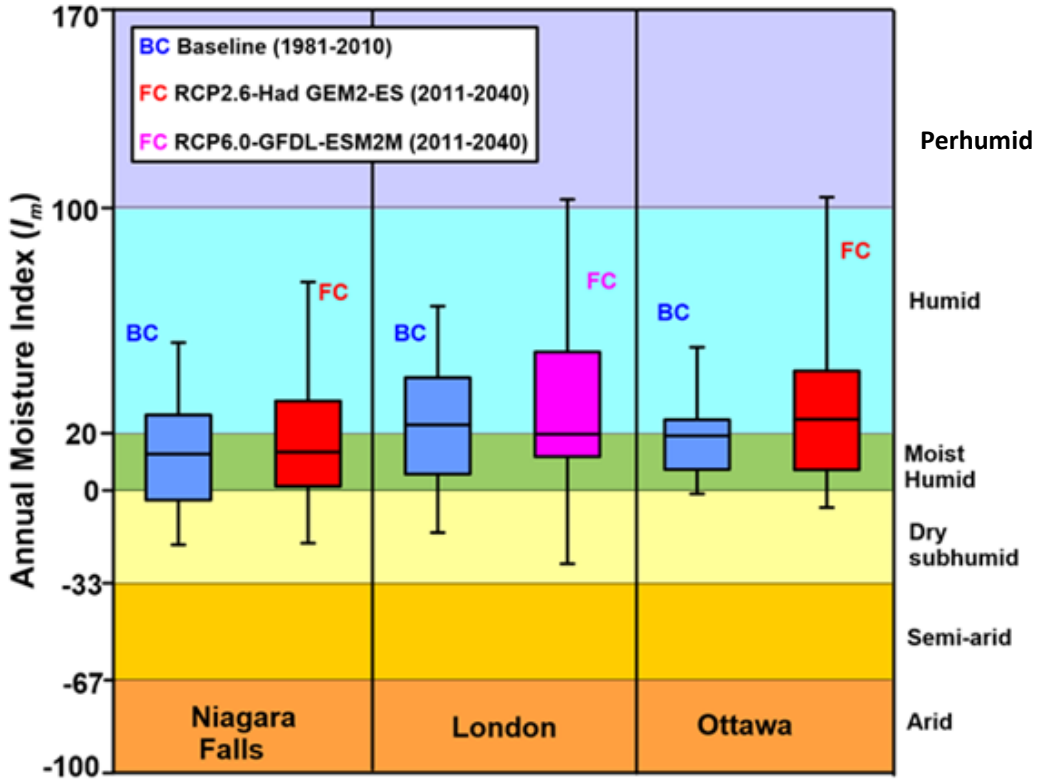

Figure 3.2 in the form of box and whisker plots for the cities of Niagara Falls, London, and Ottawa. These historical and future climate datasets described above were used in assessment

of climatic conditions at these locations. From this figure, it can be observed that in general wetter climate conditions can be expected at these three locations in the future.

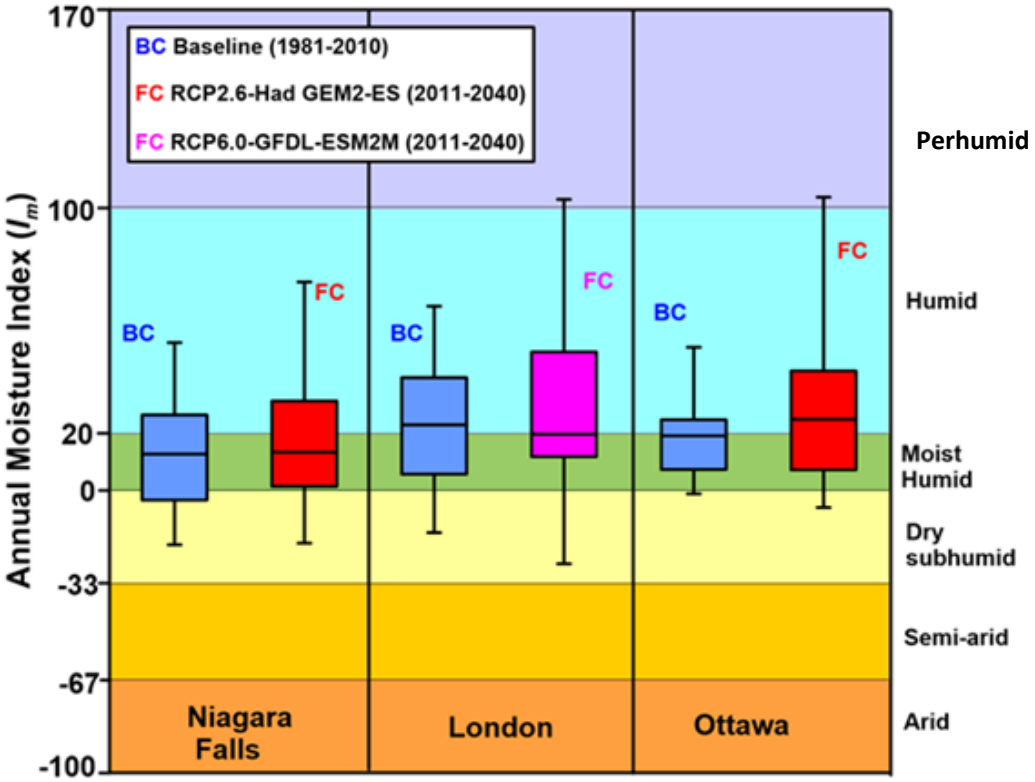

Figure 3.2 Climate Classification for Historical and Future Climate Datasets

3.2.3 Extreme Precipitation Events

Future changes in intensity and frequency of precipitation are expected to vary depending on the region and time of the year. This is in contrast to the temperature changes that are expected to increase in all locations and seasons. Considering the embankment's soil hydraulic properties, extreme precipitation events can adversely and rapidly impact the stability of slopes as large quantities of meteoric water in a short period of time can cause large increases in pore pressures within the slopes over a short period of time. The intensity and frequency of such events are expected to increase in many regions across Canada, including the southern portion

of province of Ontario (CCCR, 2019). The rainfall intensity–duration–frequency (IDF) curves are graphical representations of a mathematical function that relates the rainfall intensity with its duration and frequency of occurrence. The IDF curves can be used for many engineering purposes such as deriving design storms for slope stability assessments.

Detailed studies on historical and future IDF curves for ten different locations across Ontario have been carried out by Baninajarian (2020) and Bashir et al. (2021). These studies were reviewed in detail and relevant climate data for the cities of Niagara Falls, London and Ottawa were obtained and analyzed as part of the current research effort. Historical IDF curves for the cities of Niagara Falls, London and Ottawa were obtained from Environment and Climate Change Canada. IDF curves are available for these locations from two different sources. These two sources are the Ministry of Transportation Ontario (MTO 2018), and Ontario Climate Change Data Portal (CCDP 2018). Both sources use different methodologies for the prediction of the future IDF curves. The IDF curves are available for different return periods (2, 5, 10, 25, 100 year) and durations (5, 10,15, 30 minutes, and 1, 2, 6, 12, 24 hours). Predictions from CCDP are available for both the fourth (AR4) and fifth Assessment Report (AR5) of the IPCC (IPCC 2007, IPCC 2013). A detailed review of the data by Baninajarian (2020) indicates that in general higher intensities for shorter return periods are expected towards the end of the century. Moreover, predictions from CCDP (CCDP 2018) appear to be of higher intensities than those from MTO (MTO 2018). Therefore, in order to conduct a more conservative analysis, predictions from CCDP were analyzed further. A detailed review of the projections from CCDP indicated that the predictions for the emission scenario RCP 8.5, carried out using the regional climate model RegCM presents a worst-case scenario and was therefore selected to be used in subsequent hydrological and geotechnical modeling.

Figure 3.3 presents the historical and future intensities for the cities of Niagara Falls, London and Ottawa. These intensities are for six-hour storms for fifty- and hundred-year return periods. As described above, the historical data is from environment and climate change Canada and future predictions are from CCDP for the emission scenario RCP 8.5. It can be observed that for all the cities under consideration a considerable increase in intensities of the storms can be observed. Figure 3.4 present the percent change in historical and future intensities for the six-hour events for the three cities. It can be observed that the largest change in intensities can be observed for the City of Niagara Falls followed by the cities of London and Ottawa. The percent change in intensity for the City of Niagara Falls is expected to be as high as 140 percent. From this figure, it can also be observed that the expected increase for hundred-year event is expected to be slightly higher than the fifty-year event for the cities of Niagara Falls and London. For the City of Ottawa, the percentage increase in the future in comparison to historical value is similar for fifty- and hundred-year events.

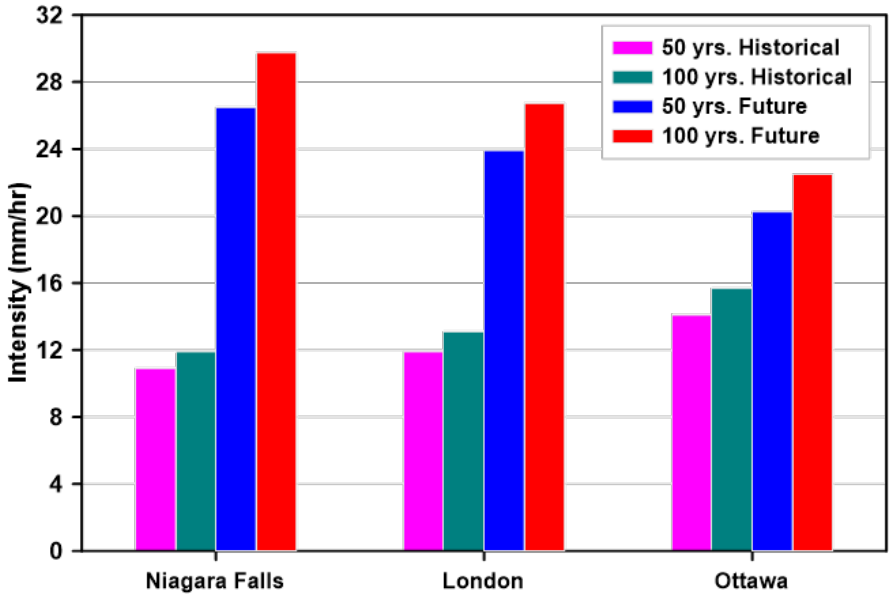

Figure 3.3 Historical and Future Precipitation Intensities for 6 hours event duration

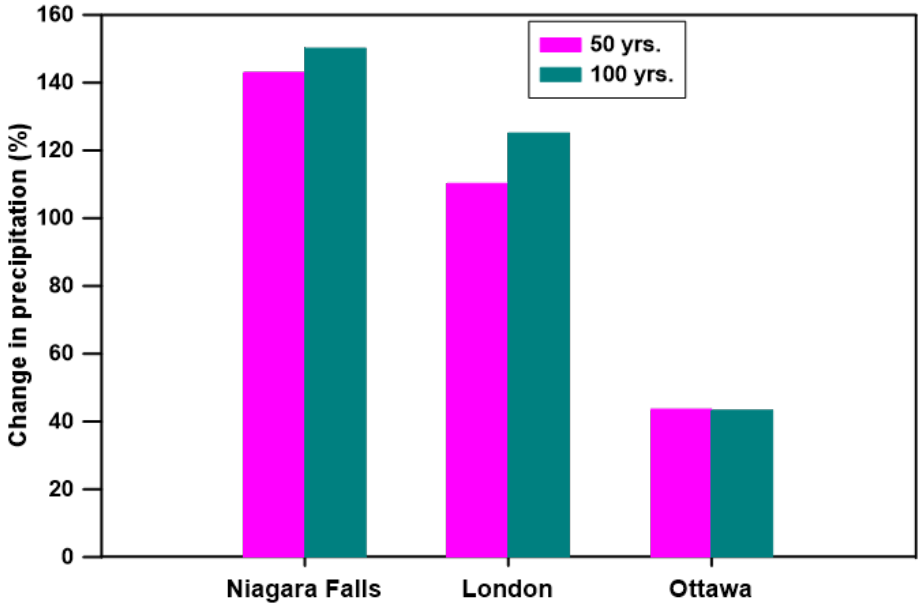

Figure 3.4 Change in Precipitation of 6-hr Precipitation Events for 50 yr and 100 yr Return Periods

3.3 Design Storm

Ideally, actual storms should be used in a hydrologic analysis (MTO, 1997). However, actual storm records are not usually available for every location. In addition, such approach is not applicable when the effects of future climate are to be studied. Therefore, establishment of synthetic storm hyetographs was considered in this study. There are several methods for generating design storm hyetographs in the literature. In some methods, a simple distribution shape is considered for a single point of the IDF curves. The simplest form is rectangular hyetographs, where a uniform intensity is used throughout the storm duration (Prodanovic & Simonovic, 2004). However, this method has been reported to underestimate the total precipitation volume of rainfall events for some hydrological analyses (Veneziano and Villani,

1999). Alternatively, geometric forms such as triangular hyetographs (e.g., Yen and Chow (1980)) or linear/exponential hyetographs (e.g., Watt et al. (1986)) have also been proposed. As an alternative of using a single point on an IDF curve, methods have been proposed that use the entire set of duration-intensity values for a particular return period and duration (e.g., Keifer and Chu (1957) and USACE (2000)). Among these methods, method proposed by Keifer and Chu (1957), known as the Chicago design storm, has been widely incorporated in Canadian practice, because it can be readily derived from available rainfall IDF relationships and partly because of limited alternative approaches (Marsalek, 1982; Marsalek & Watt, 1984). This method has also been suggested by Ministry of Transportation of Ontario to be applied for assessment of the storm impacts on the drainage systems (MTO, 1997). In this study, the Chicago method was applied for providing intensity distribution over time for historical and future extreme precipitation events.

The Chicago method's equations can be analytically derived from an IDF analytical expression:

$$i = \frac{a}{(b+t_d)^n} \qquad \text{Equation 3.2}$$

where i is the rainfall intensity, t_d is the duration, a, b and n are the constants that represent local conditions and the return period and are dependent on the units employed, the volume equation associated with the intensity of IDF for each duration can be given by:

$$V_t = \frac{at_d}{(b+t_d)^n}$$ Equation 3.3

Assuming i_t is the intensity as a function of time (instead of duration), the integration of i_t over time is equal to rainfall volume:

$$\int_0^{t_d} i_t dt = V_t = \frac{at_d}{(b+t_d)^n}$$ Equation 3.4

Therefore, i_t can be analytically derived from the above equation as:

$$i_t = \frac{a[t(1-n)+b]}{(b+t)^{n+1}}$$ Equation 3.5

According to the Chicago method, the asymmetry of the hyetograph can be adjusted by a parameter r (where $0 < r < 1$) which represents the ratio of the time of peak intensity (t_p) divided by the storm duration (t_d). As a result, the $i_t = \frac{a[t(1-n)+b]}{(b+t)^{n+1}}$ Equation 3.5 can be rewritten for before and after intensity peak as follows:

$$i_{t,b} = \frac{a[\frac{t_b}{r}(1-n)+b]}{\left(b+\frac{t_b}{r}\right)^{n+1}} \qquad (t_b = t_p - t \qquad 0 \le t \le t_p)$$ Equation 3.6

$$i_{t,a} = \frac{a[\frac{t_a}{1-r}(1-n)+b]}{\left(b+\frac{t_a}{1-r}\right)^{n+1}} \qquad (t_a = t - t_p \qquad t_p \leq t \leq t_d) \qquad \text{Equation 3.7}$$

The value of r is usually derived from existing rainfall records. The method involves calculating the mean values of mass antecedent rainfall and the mean location of the peaks for various rainfall durations for a series of excessive rainfall events. The process is lengthy and subject to interpretation. A *r* value of 0.38 has been suggested for all of the province of Ontario (MTO, 1997).

Figure 3.5 shows an example of the design storms developed based on future IDF curve for a 100-year return period and 6-hour duration for the City of Niagara Falls. The values of constants a, b and n are 718.92, 2.65 and 0.66 for Historical and 1943.94, 7.30 and, 0.72 Future storms respectively. It should be noted that using a very small-time step with the Chicago hyetograph can result in an unrealistic high peak rainfall intensity. Herein, time step between 1 to 10 minutes were applied for developing different design storms. The design storms were developed for six-hour durations for the 50- and 100-year return periods based on the historical and future IDF curves.

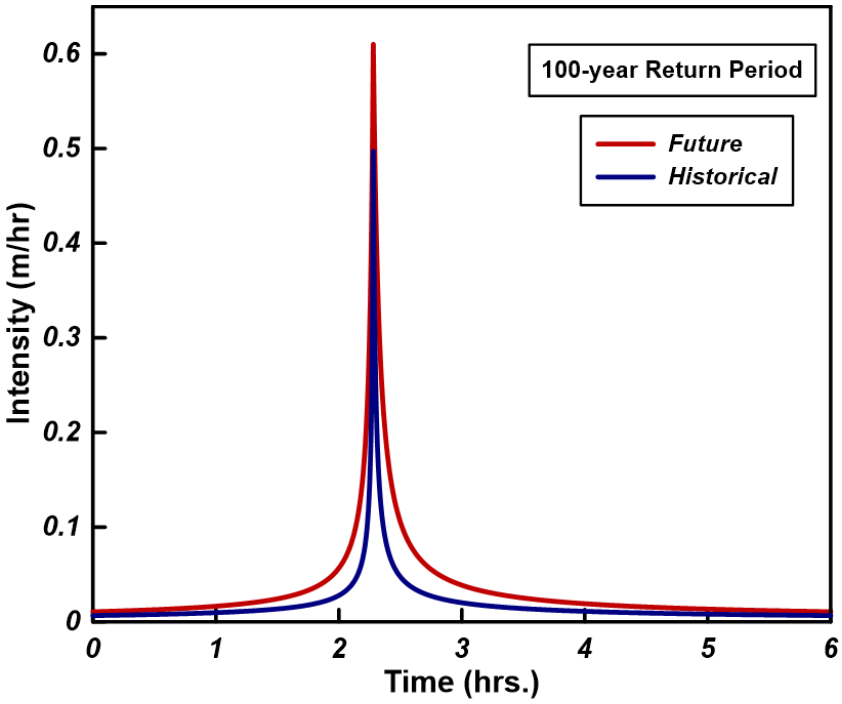

Figure 3.5 IDF Curves - Historical and Future Storm - 6 hours Duration - Niagara Falls

Chapter 4: Numerical Modeling Details

4.1 Introduction

Numerical simulation of climate change impact on slope stability requires a multi-disciplinary approach. This includes a climate model to provide high-resolution future climate dataset as well as a hydrological model to simulate variably saturated flow with soil-atmosphere interaction. Further, a proper geotechnical model is required for slope stability assessment considering the effects of suction on the shear strength of the soil.

In this chapter, the geometry of the models used in the case studies and relevant unsaturated hydraulic and geotechnical parameters, are presented. Details of the initial and boundary conditions of the numerical models are also presented.

The main focus of this research is on the Local Factor of Safety (LFS) assessment, as described in Chapter 2: . Therefore, methodology of stability assessment using the field of LFS (Lu et al., 2019) is discussed in this Chapter. In this study, HYDRUS (2D/3D) (Šimůnek et al. 2006) was used for analyzing the variation of water distribution in the embankment subjected to historical and future climate data. To compute the field of LFS, Cube module of the HYDRUS (2D/3D) software package was used. This supplemental module computes the soil stresses under gravity (i.e., moist unit weight) and effective stress (i.e., suction stress). For two-dimensional analysis this module uses finite element formulation for linear elasticity analysis. The pore pressure distribution obtained from HYDRUS (2D/3D) seepage analysis is used in Cube to calculate the effective stresses and the field of LFS, as discussed in Chapter 2: .

In addition to the above-mentioned coupled hydro-mechanical model, conventional LEM, FEM-based LEM, and elasto-plastic FEM are also briefly described. It should be noted that the elasto-plastic FEM method that employed in this research, can assess the potential failure area

within the slope and stress-strain behaviour of soils is not modeled. These approaches were used for the validation of the LFS method. All the models in this research use hydro-mechanical coupling. In other words, pore pressure distribution obtained from the seepage analysis at each step is introduced in the geotechnical models to assess the stability of the embankment slope.

4.2 Hydro-Mechanical Models

4.2.1 Variably Saturated Flow Analysis

HYDRUS (2D/3D) is a finite element software that numerically solves the Richards' equation for analysis of water flow in the variably saturated soils. The software utilizes a system-dependent boundary condition that controls the maximum amount of water that can either evaporate or enter the soil-atmosphere boundary to estimate actual evaporation and the resulting influx of meteoric water into the embankment surface. HYDRUS (2D/3D) (Šimŭnek et al. 2006) was employed to analyze the long-term variation of slope moisture conditions. This software is capable of simulating the movement of water, heat, and multiple solutes in the variably saturated media using the finite element method. HYDRUS 2D is computationally efficient and is capable of running long-term simulations in manageable time frames in an efficient manner (Pk et al. 2018).

4.2.2 Slope Stability Analysis – LFS Method

The effect of climate change on the stability of embankments was quantified by estimating a field of LFS using a coupled finite element in-situ stress analysis and a variably unsaturated flow analysis. The precipitation will cause variation in the soil embankment moisture content and soil suction. The Cube module of the HYDRUS (2D/3D) can couple the variably saturated flow and the in-situ soil stress in the field of FEM, at the same time (Lu et al., 2019). This approach determines the field of local factor of safety based on elastic finite element analysis. The method

can be used not only to identify the slope instabilities, but also to determine the distribution of the zones with lower factor of safety within the slope.

The slope stability assessment using LFS can be summarized, as follows:

- In situ stress analysis, using a two-dimensional finite element formulation;
- Calculation of pore water distribution within the slope for each time step from the seepage analysis in HYDRUS (2D/3D);
- Calculation of field of suction stress for each time step using the Cube Module based on pore pressure distribution;
- Estimation of field of LFS based on minimum and maximum principal effective stresses and soil strength parameters, as described in the Chapter 2: ; and,
- Calculation of total area of Local Factor of Safety (A_{LFS}) using a purposely written Fortran code.

Although LFS contour maps produced by the Cube Module present a general display of slope stability conditions, a quantitative LFS indicator is required particularly when the variation of LFS over time is of interest. Bagheri et al. (2019) defined a slope stability indicator based on the area of LFS below a certain threshold in the model cross section. The LFS contours with relevant factor of safety can be assessed in Cube module. The area of embankment in which LFS is less than unity ($A_{LFS}<1$) can be considered as the indicator of the potential failure mass. The variation of $A_{LFS}<1$ over time was estimated using a Fortran code (Bagheri , A., 2019). This code imports the mesh coordinates and nodal values of LFS in a user selected area of the embankment over the course of the entire simulation. The code has the capability to sum up the area of the embankment in which the LFS is less than or equal to a user defined threshold value such as 1.0. This greatly enhances the analysis, as the temporal changes in area of failure mass can be tracked.

4.2.3 Other Slope Stability Methods

The use of finite element methods for slope stability analyses is becoming increasingly common. One of the main advantages of the finite element method is that stress and strain fields can be calculated without simplifications that are normally used in the conventional limit equilibrium method (LEM) of slices. In the conventional LEM methods, the sliding surfaces are assumed, and the initiation of failure cannot be studied, as discussed in the Chapter 2: of this thesis. The finite element method, apart from estimating stress and strain field, can also be used to estimate a factor of safety which is a widely used indicator for slope stability assessments. Some of the common approaches to determine factor of safety based on the conventional and finite element analysis are as follows:

- The widely used limit equilibrium software SLOPE/W together with seepage software SEEP/W was also used in this research. Both of these programs are modules of a software suite called GeoStudio (Geo-Slope International Ltd. 2016) and can be coupled easily. The coupling ensures the continuous calculation of FOS of slopes by SLOPE/W for each time step, for which pore pressure distribution is available from the seepage analysis by SEEP/W. Morgenstern-Price method (Morgenstern and Price 1965) that considers both the static force and moment equilibrium in limit equilibrium analyses was used in this research. The strength due to suction in unsaturated soil was estimated based on two stress state variables approach using the method by Vanapalli et al. (1996) as discussed in Section 2.3.
- Finite Element Limit Equilibrium Method: The finite element limit equilibrium analyses were carried out in this research by coupling the SIGMA/W and limit equilibrium software SLOPE/W. Both software are modules of GeoStudio (Geo-Slope International Ltd. 2016) and can be coupled easily. For this type of analysis, the stress distribution calculated by SIGMA/W

which is a stress-strain finite element module of the widely used commercial software package GeoStudio (Geo-Slope International Ltd. 2016).is used in SLOPE/W to determine the safety factors along the potential slip surfaces. In this method, shape and location of the critical slip surface corresponding to the minimum FOS can be identified. In contrast to conventional LEM, the field of stresses is calculated by using finite element analysis (Fredlund and Scoular, 1999; Liu et al., 2020).

- Elasto-plastic Finite Element Analysis: Local instabilities may not necessarily lead to global failures that are routinely identified by the LEM. Instead, local instabilities can be identified from yield points by carrying out an elasto-plastic finite element analysis. In this method, slope stability is assessed by taking into consideration stress concentration without assumptions or identification of potential failure surfaces. Elasto-plastic finite element analyses were carried out using SIGMA/W, Mohr-Coulomb yield criterion was used in these analyses. The Mohr-Coulomb parameters had the same values as used in limit equilibrium analysis.

For validation purposes, the results of LFS method were compared to these three different approaches i.e., LEM, finite element limit equilibrium analyses and elasto-plastic finite element analyses.

4.3 Embankment Geometry and Material

A typical Ontario highway embankment profile as shown on Fig. 4.1 has been considered for this study. According to OSPD 202.010, embankments without berm, can be constructed to a maximum height of 8m in the province of Ontario. Therefore, in this research, the height of embankment is considered to be 8 m with side slopes of 2 horizontal to 1 vertical (2H:1V).

Moreover, a 3m wide unpaved shoulder on the top of embankment is also considered. Due to symmetrical geometry of the typical highway embankments, only one half of the embankment profile is simulated in the numerical models. In order to minimize the influence of the side boundary conditions, the model horizontal length was extended three times the embankment height, to the right of toe of the slope. This is in line with the recommendation by Rahardjo et al. (2010). The water table is conservatively assumed at the natural ground surface that is 4 m below the level of slope toe (i.e., at the embankment base).

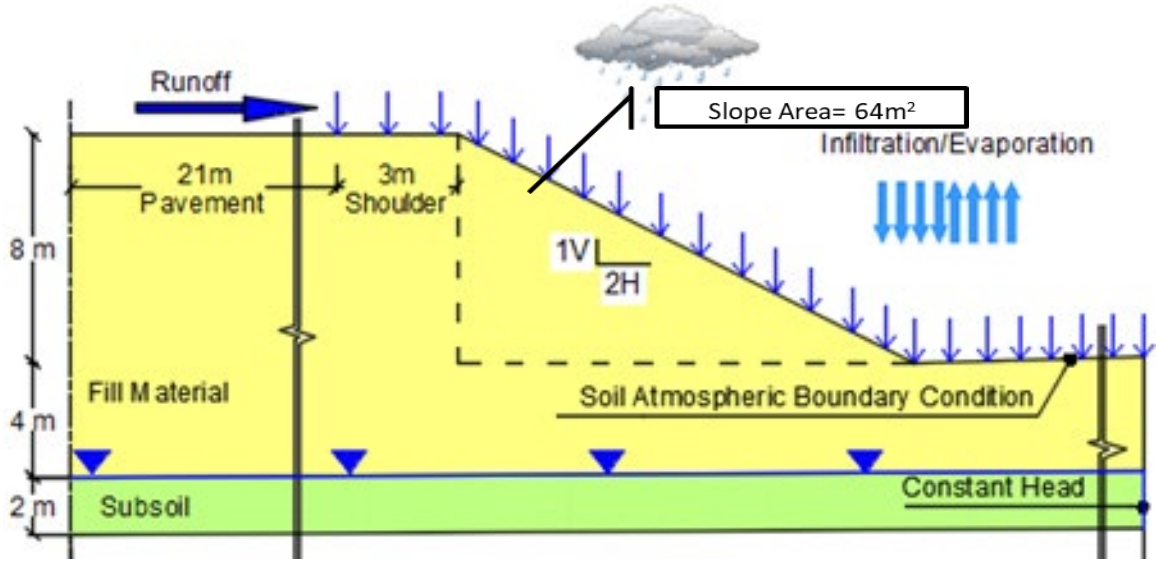

Figure 4.1 Geometry of the Highway Embankment used in the hydrological and geotechnical modeling

It is understood that select subgrade material (SSM) is often used in embankment construction across Ontario (Bashir et al., 2021). Silty sand and sandy silt materials are considered as the embankment fill in this study. Hydraulic properties, namely soil water characteristic curves (SWCC) and the unsaturated hydraulic conductivity function (HCF) are required to simulate flow in variably saturated conditions (Lu & Kaya, 2013). The SWCC relates matric or total suction

(soil-water potential) to water content and can be used to predict the HCF of the unsaturated soils. The HCF provides the relation between hydraulic conductivity and soil water content (Mualem, 1976). The mathematical model suggested by van Genuchten (1980) was used to represent the soil water characteristic curve (SWCC). This function is as follows:

$$\theta = \frac{(\theta_s - \theta_r)}{[1+(|\alpha h|)^n]^m} + \theta_r \qquad \text{Equation 4.1}$$

This function relates soil volumetric water content (θ) to matric suction (h) for a given saturated (θ_s) and residual water content (θ_r). The value of θ_s is equal to the soil porosity for no air entrapment. The empirical coefficients used as the fitting parameters (i.e., α and n), are related to the inverse of the air entry value and soil pore-size distribution and $m = 1 - \frac{1}{n}$ is related to the asymmetry of the van Genuchten model (Taban et al., 2017). Measurement of hydraulic parameters is usually limited to small number of laboratory or field tests, due to cost and schedule constraints (Bashir et al., 2020). The van Genuchten (1980) soil hydraulic parameters for the sand silt materials considered in this research are presented in Table 4.1 and resulting SWCCs are plotted on Figure 4.2. These parameters were estimated by Baninajarian (2020) and Bashir et al. 2021 and the estimation details can be found in these references. It should be noted that the HCF was determined from SWCC using the van Genuchten-Mualem approach (Mualem 1976, and, van Genuchten 1980) as follows:

$$K(h) = K_s S_e^{\ell} \left[I - \left(1 - S_e^{1/m} \right)^m \right]^2 \qquad \text{Equation 4.2}$$

ℓ is commonly assumed to be 0.5 and the effective saturation, S_e, is computed as follows:

$$S_e = \frac{\theta - \theta_r}{\theta_s - \theta_r}$$ Equation 4.3

,

Table 4.1 van Genuchten (1980) SWCC Parameters and Saturated Hydraulic Conductivity Values for Sand and Silt

Material	θ_s	θ_r	α (1/cm)	n	K_s(cm/hour)
Sand	0.32	0.05	0.06	1.53	3.6
Silt	0.45	0.07	0.02	1.41	0.45

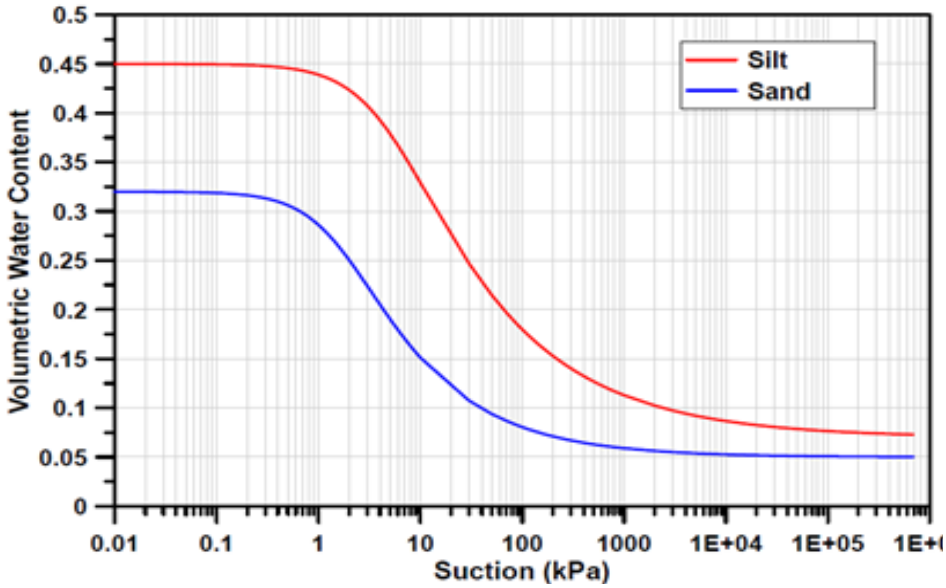

Figure 4.2 Soil Water Characteristics Curves for Selected Material

The Embankment fill materials for MTO, and majority of transit and transportation projects in Ontario are to be placed and compacted in accordance with the provincial standards, OPSS 206 and OPSS 501 (Baninajarian 2020). An effective friction angle of 34° and 32° is assumed for compacted sand and silt materials, respectively. For finite element analyses using Cube, the value of Poisson's ratio that controls the development of horizontal stresses is assumed to be 0.3 and

0.35 for the sand and silt, respectively. The selected values for dry unit weight, porosity and saturated unit weight are presented in Table 4.2. These values were selected based on the MTO specification and a detailed study carried out by Bashir et al. (2020).

Table 4.2 Dry and Saturated Unit Weights, and Porosity

Material	**Dry unit weight (kN/m^3)**	**Porosity**	**Saturated unit weight (kN/m^3)**
Sand	17.5	0.33	20.7
Silt	14.7	0.44	19.0

4.4 Initial Conditions

It is a common practice to assume hydrostatic pore pressure distribution as the initial condition for the numerical simulation of a slope subjected to rainfall (e.g., Robinsonet al. 2017; Pket al. 2018). However, the hydrostatic conditions are a special and rare case in reality at the field scale when thermodynamic equilibrium is reached (Lu and Godt, 2013). Initial modeling results suggested that for a typical embankment considered in this research, assuming the hydrostatic condition results in saturation within slope area to be equal to 30% and 45% for sand and silt materials respectively.

Baninajarian (2020) and Bashir et al. (2021) used HYDRUS 2D for analyzing the long-term variation of slope moisture conditions under historical and future long-term climatic conditions. For each location, historical and future long-term climate data, as described in Chapter 3 was used for soil–atmosphere modelling of embankments with sand and silt materials. A statistical analysis on the daily variation of average water content in the slope area of the embankment was carried out by Baninajarian (2020). Different percentiles of the slope moisture conditions estimated for

sand and silt embankments were extracted for the cities of Niagara Falls, London and Ottawa and were used in the current research effort.

In this research, degrees of saturation corresponding to the 50th and 90th percentiles (P 50% and P 90%) were considered as representatives for the normal range and above-normal range of saturation. These percentile saturations were used to define the initial conditions in slope stability analysis for extreme precipitation events. The degree of saturation corresponding to the 50th and 90th percentiles for the cities of Niagara Falls, London and Ottawa for sand and silt embankments are shown in Table 4.3 and Table 4.4, respectively. It can be observed that for many instances the intermediate percentile values of P 50% and P 90% are expected to increase in the future. It should also be noted that in almost all instances the maximum saturations are expected to be higher in the future than the historical values (Baninajarian 2020).

Table 4.3 Degree of Saturation - Sand Embankments

Location	**50th Percentile used for Initial Condition (IP 50%)**		**90th Percentile used for Initial Condition (IP 90%)**	
	Historical	**Future**	**Historical**	**Future**
Niagara Falls	57.3	56.9	64.7	64.9
London	57.5	57.3	65.7	67
Ottawa	56.9	57.6	64.8	66.5

Table 4.4 Degree of Saturation - Silt Embankments

Location	**50th Percentile used for Initial Condition (IP 50%)**		**90th Percentile used for Initial Condition (IP 90%)**	
	Historical	**Future**	**Historical**	**Future**
Niagara Falls	73.9	74.1	82.3	81.8
London	75.5	75.2	84.38	85.1
Ottawa	74.1	75	82.2	83.6

4.5 Boundary Conditions

4.5.1 Hydraulic Boundary Condition

The boundary conditions for the hydrological model are shows on Figure 4.3. It can be observed that a no-flow boundary condition was applied at the pavement, on the left-hand side, and bottom of the embankment model. On the right-hand side of model, constant head boundary corresponding to the depth of 4 m below the toe of the slope was applied. The remainder of the right-hand side boundary was assumed to be seepage face. A flux boundary consisting of design storm records was applied at the soil-atmosphere interface. The relevant location of the boundary conditions can be seen on Figure 4.3.

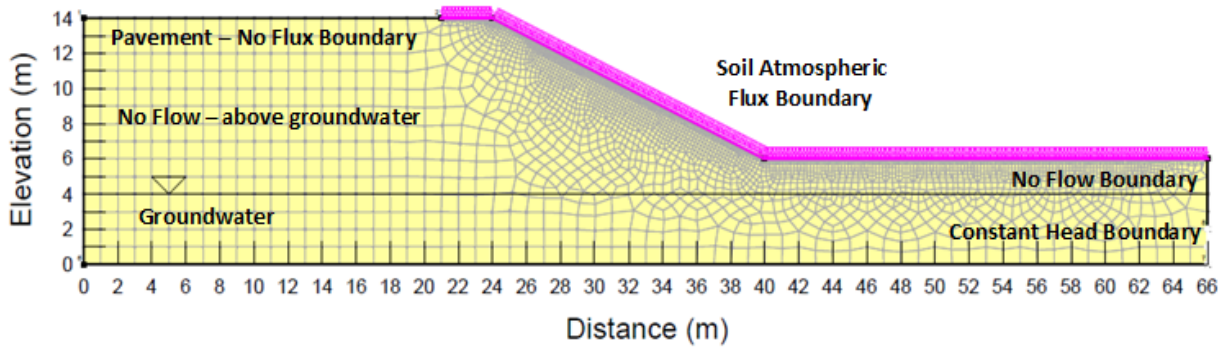

Figure 4.3 Hydraulic Boundary Conditions

4.5.2 Mechanical Boundary Condition

To compute the field of in situ stresses, Cube module of the HYDRUS 2D/3D software package was used. In situ stress analysis was carried out with the left and right boundaries free to move in the vertical direction, while the bottom boundary is fixed in both vertical and horizontal directions as shown on Figure 4.4.

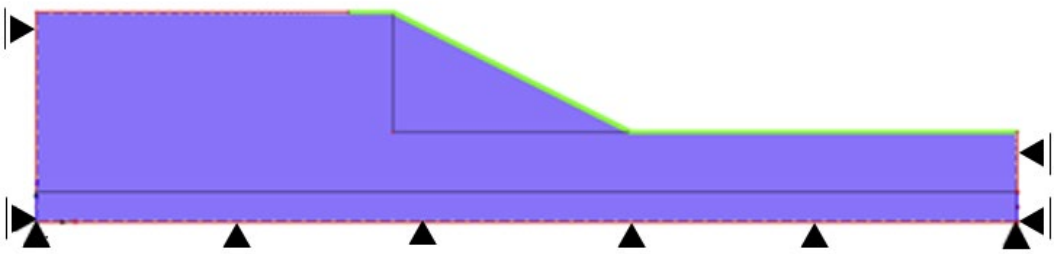

Figure 4.4 Mechanical Boundary Conditions

Chapter 5: Findings and Discussion

5.1 Introduction

In this chapter, the findings from Local Factor of Safety (LFS) analyses for typical sand and silt embankments under historical and future climate conditions for the cities of Niagara Falls, London, and Ottawa in the province of Ontario are discussed. Results for embankments in the City of Niagara Falls for historical and future extreme precipitation events are discussed in detail. The similar results for London and Ottawa are presented in Appendix B, and the comparison of results for all the three cities are summarized in Section 5.6.

The effect of climate change on the stability of earth fill embankments is quantified by estimating the field of Local Factor of Safety (LFS). For estimation of LFS, a coupled hydro-mechanical model equipped with soil atmospheric boundary condition using variably saturated flow formulation is used. The effect of moisture content variation on the effective stress and shear strength is considered and simulated using the suction stress state concept within the unsaturated soil mechanics framework.

Moreover, the results from LFS model are validated against three other slope stability methods, namely, conventional limit equilibrium method (LEM), elasto-plastic finite element method (FEM), and finite element based LEM. For the finite element based LEM, the stress distribution (linear elastic) within the slope is computed for the gravity load and is used for calculation of the factor of safety. In the finite element analysis with the elasto-plastic approach, the area of the yielded mass is compared with the area within the slope mass with LFS<1. The validation results are presented for both sand and silt embankments for the City of Niagara Falls.

Embankment's response to the historical and future extreme events, are studied using the LFS method. The results are presented in terms of changes in moisture content and suction stress at

selected times. Furthermore, the LFS evaluation of sand and silt embankments due to the impact of climate change in three cities of Niagara Falls, London and Ottawa is presented in terms of temporal variation of slope area with LFS<1 from the start of the storm to 18 hours following the end of the extreme precipitation event.

5.2 Numerical Model Validation

For the LFS method validation and comparison, the stability of sand and silt embankments was assessed based on a 6-hour future design storm for the City of Niagara Fall with a 100-year return period. The results from LFS method are then compared to the results of three other slope stability analysis approaches i.e., the conventional LEM, the finite element LEM, and elasto-plastic finite element analysis. In general, all classical LEM methods calculate ratio of the available shear strength to the shear stress required for equilibrium along the prescribed failure surfaces.

In a conventional LEM approach such as Morgenstern & Price (1965), the forces acting on each slice are determined, such that all slices are in force equilibrium and moment equilibrium and have the same factor of safety (Krahn et al., 2003). The defined stress distribution along a slip surface is not completely accurate because the field of stress-strain relationship is not considered in conventional LEM to calculate factor of safety Finite (GEO-SLOPE International Ltd.).

In finite element LEM, the stress field is determined through a finite element analysis, which in this study has been carried out using SIGMA/W and then the stresses are inputted to SLOPW/W to calculate the safety factors.

Figure 5.1 and Figure 5.2 present the critical slip surface and the minimum global factor of safety using conventional and finite element limit equilibrium methods for sand and silt embankments, respectively. It should be noted that for both the analyses, pore pressure distribution

at the end of 6 hr storm simulated using SEEP/W, was inputted into the SLOPE/W and SIGMA/W. It can be observed that minimum factors of safety are greater than one for both sand and silt embankments using the conventional and finite element method based LEM. It can also be observed that for both sand and silt embankments, the finite element method based LEM predicts lower factor of safety at shallower depth comparing to the conventional LEM FS results.

In limit equilibrium analyses, global factor of safety (FOS) represents the stability condition of the entire slope. The limit equilibrium approach is not effective in identification of potential local instabilities which is a typical failure mechanism in slopes subjected to extreme precipitation events (Pk et al. 2018). Potential local instability can be identified using finite element analysis with elasto-plastic constitutive models. For this purpose, a set of adjacent yield points from a stress-strain analysis can be utilized to characterize the local instabilities. Figure 5.3 and Figure 5.4 illustrate the results of elasto-plastic finite element analysis for the sand and silt embankments respectively. Consistent with LEM analyses described above, these results are also for pore pressure distribution at the end of the 100-year future extreme precipitation event. Set of adjacent yield points are identified on these figures.

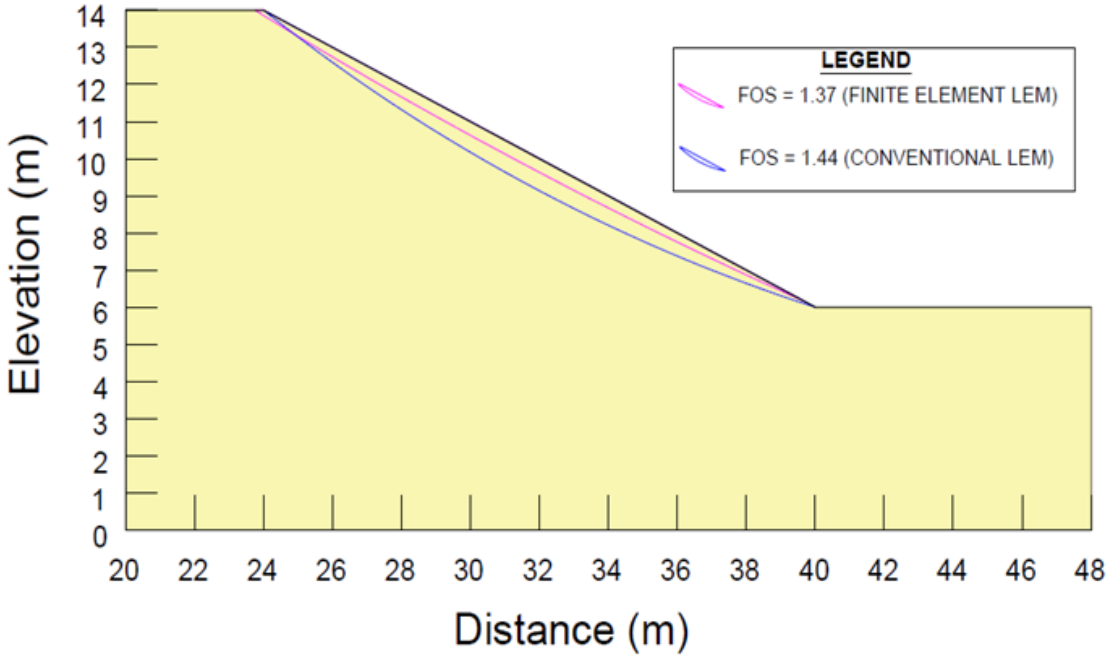

Figure 5.1 Conventional vs Finite Element LEM- Sand Embankment

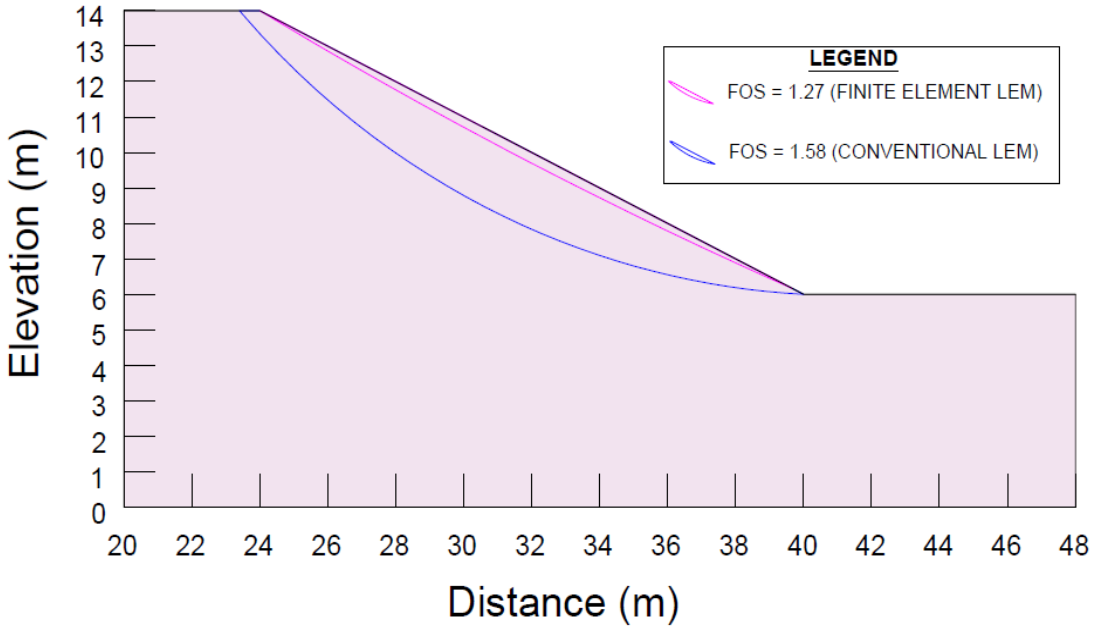

Figure 5.2 Conventional vs Finite Element LEM- Silt Embankment

It can be observed that for both the sand and silt embankments, a shallow area of yield points can be clearly seen in the slope area of the embankment. It should also be noted that in the assessments using the elasto-plastic material, the plastic points are not necessarily an indication of the slope failure mechanism. For example, a local zone of plastic points obtained from numerical analysis can be kinematically stable and may not necessarily cause progressive slope failure.

In the LFS method, a local factor of safety is calculated for every point in the domain. Thus, a map of LFS contours, that trace lines of equal LFS values can be obtained. This method can be used to estimate the potential local instabilities by mapping the contour of LFS=1.0. Figure 5.3 and Figure 5.4 also show the contour of LFS=1.0 for sand and silt embankments, respectively. A review of these figure indicates that the LFS contours appear to be in good agreement with the yield points zone obtained from elasto-plastic finite element analysis. The results illustrated on Figure 5.3 and Figure 5.4 also confirm that shallow surficial failures that are not identified by either the conventional or finite element LEM based analysis can be captured by utilizing the local factor of safety approach. It should be noted that LFS method can be used to develop contour map for any desired LFS value. As an example, the contour map of LFS=1.3 are also shown on Figure 5.3 and Figure 5.4 for sand and silt embankments, respectively.

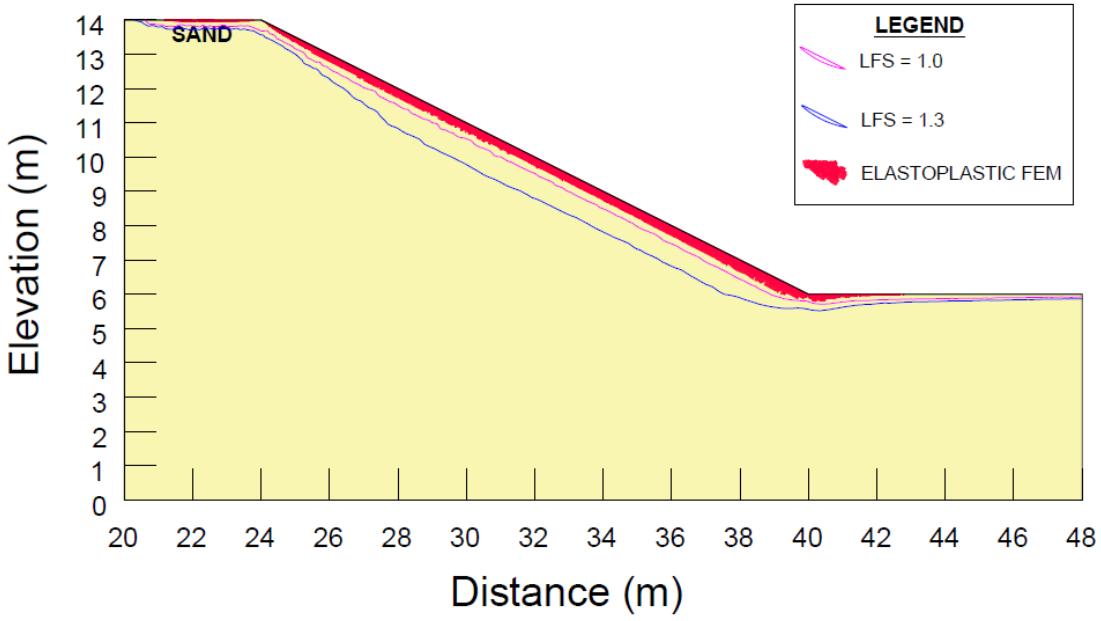

Figure 5.3 LFS field vs Yield points- Sand Embankment

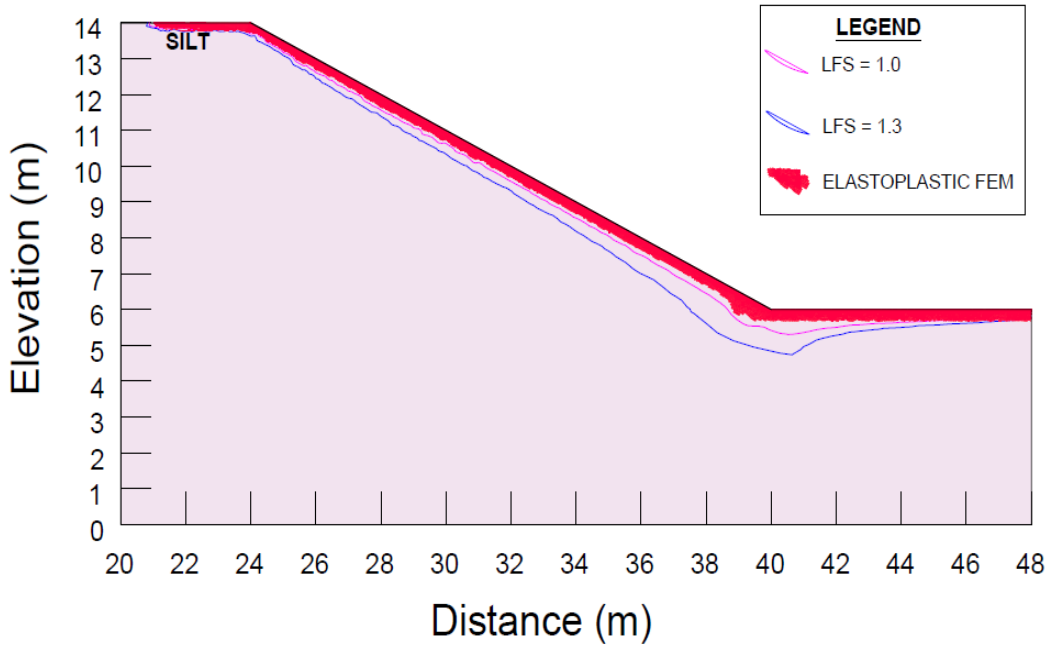

Figure 5.4 LFS field vs Yield points- Silt Embankment

.

5.3 Embankment Response to Extreme Events

In this section, the response of sand and silt embankments in the City of Niagara Falls to extreme precipitation events is presented and discussed. The response is presented in terms of temporal variation of suction stress, moisture content, and field of LFS at the start middle and end of the extreme precipitation events. The initial conditions corresponding to 50th percentile of long-term slope moisture conditions are used, as described in Chapter 4: . The analysis is carried out for the 6-hour future extreme event with a 50-year return period. The following results are presented at the initiation of the precipitation event, end of precipitation end (6 hours after the initiation) and 18 hours following the end of the extreme precipitation event.

5.3.1 Moisture Content Variation During an Extreme Precipitation Event

Figure 5.5 shows the moisture content distribution within the slope area of embankment at the start, end, and 18 hours after the extreme precipitation event (i.e., Time 0, 6 and 24 hrs.). It can be observed that at the onset of the extreme precipitation event, the water content in the near surface sloped area of the embankment varies between approximately 15% and 17% which is about 50% of complete saturation (i.e., θ_s=32%) for sand. It can also be observed that at the end of extreme precipitation event, an almost completely saturated region develops in the top part of the slope area. The depth of this completely saturated region is approximately 1.25 metres and appears to be uniformly distributed over the top of slope area. This leads one to conclude the depth effected by extreme precipitation event at the end of the event is limited to approximately 1.25 m. The moisture content distribution, 18 hours after the end of precipitation event shows that the moisture content is now reduced to 22% within the 0.2 m of slope surface. However, higher moisture content from 0.2 m below slope surface to approximately 1.25 m below ground along the slope surface can still be observed. Farther from the toe of the slope, higher saturation within depth can

be observed indicating that from the end of precipitation (i.e., Time 6 hrs) until 18 hours after the end of extreme event, higher saturation of approximately 25% has penetrated to a depth of approximately 2m below ground surface.

The moisture content variation for the same extreme precipitation event for silt embankment is illustrated on Figure 5.6. All other conditions such as initial condition and return period are similar to the sand embankment conditions as described above. Based on results presented on Figure 5.6, at the start of the extreme precipitation event, the top 0.35m of slope area is at a moisture content of 20%. This translates to a saturation, close to 50%, as the saturated water content of silt is assumed to be 45%. The moisture content distribution at the end of the extreme precipitation event indicates that the a near saturated zone of 0.35m develops near the surface. In this zone the moisture ranges from approximately 42% to 45%.

The comparison of moisture content distribution for sand and silt embankments indicates that the depths of moisture penetration, at end of extreme event are not similar for sand and silt embankment (Figure 5.5 (b) and Figure 5.6 (b)). This is related to the difference in hydraulic properties of sand and silt materials i.e., soil material conduction and retention properties. Water retention of soils is related to the soil particle-size composition that increases from sandy to more fine sized soils, (Bolotov et al., 2019). Water conduction is also related to the soil particle-size composition and decreases from sandy to more fine sized soils. Silt has lower hydraulic conductivity and generates more runoff for a storm of similar intensity, resulting in lower net infiltration.

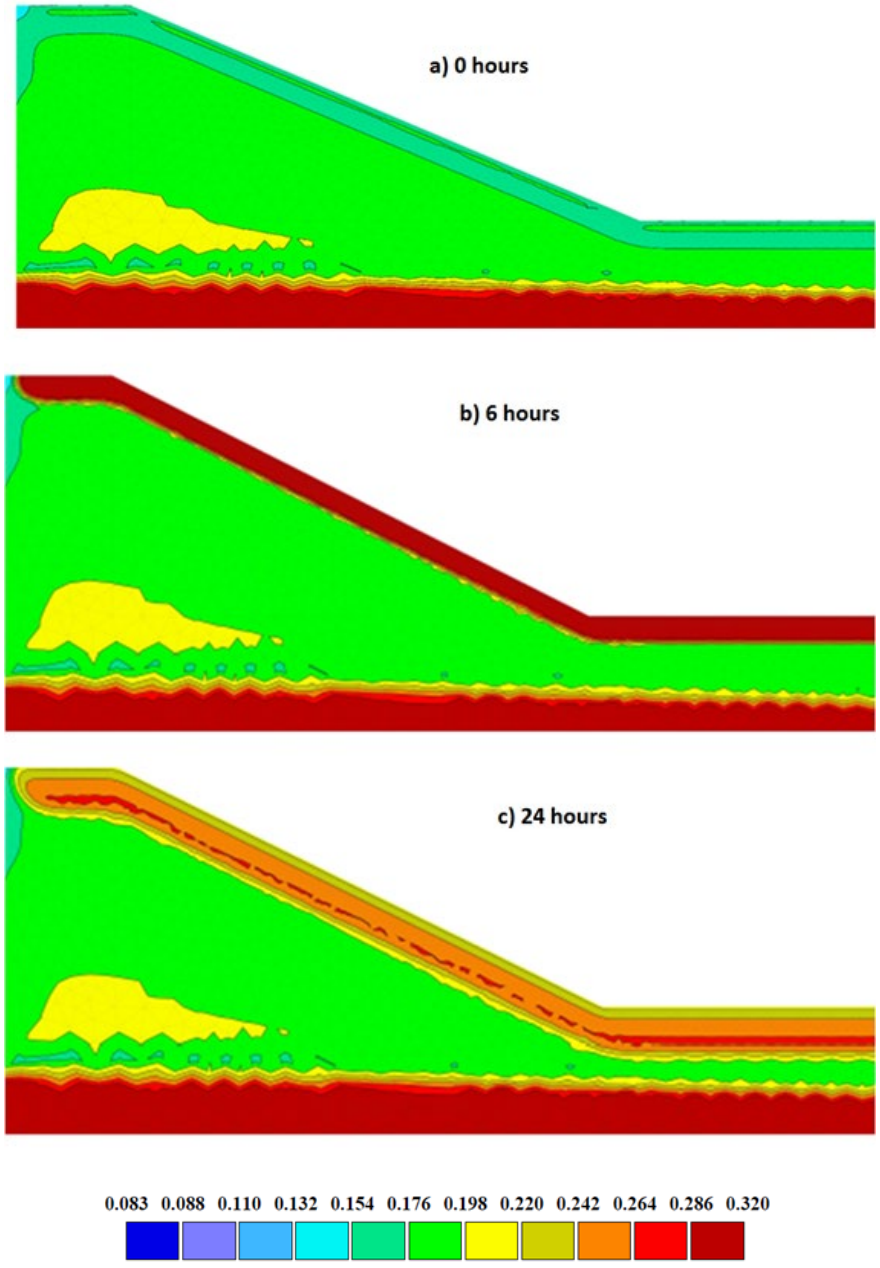

Figure 5.5 Moisture Content -Sand Embankment -Niagara Falls – Fut. IP 50% - T50 yr. Time 0, 6 and 24 hrs.

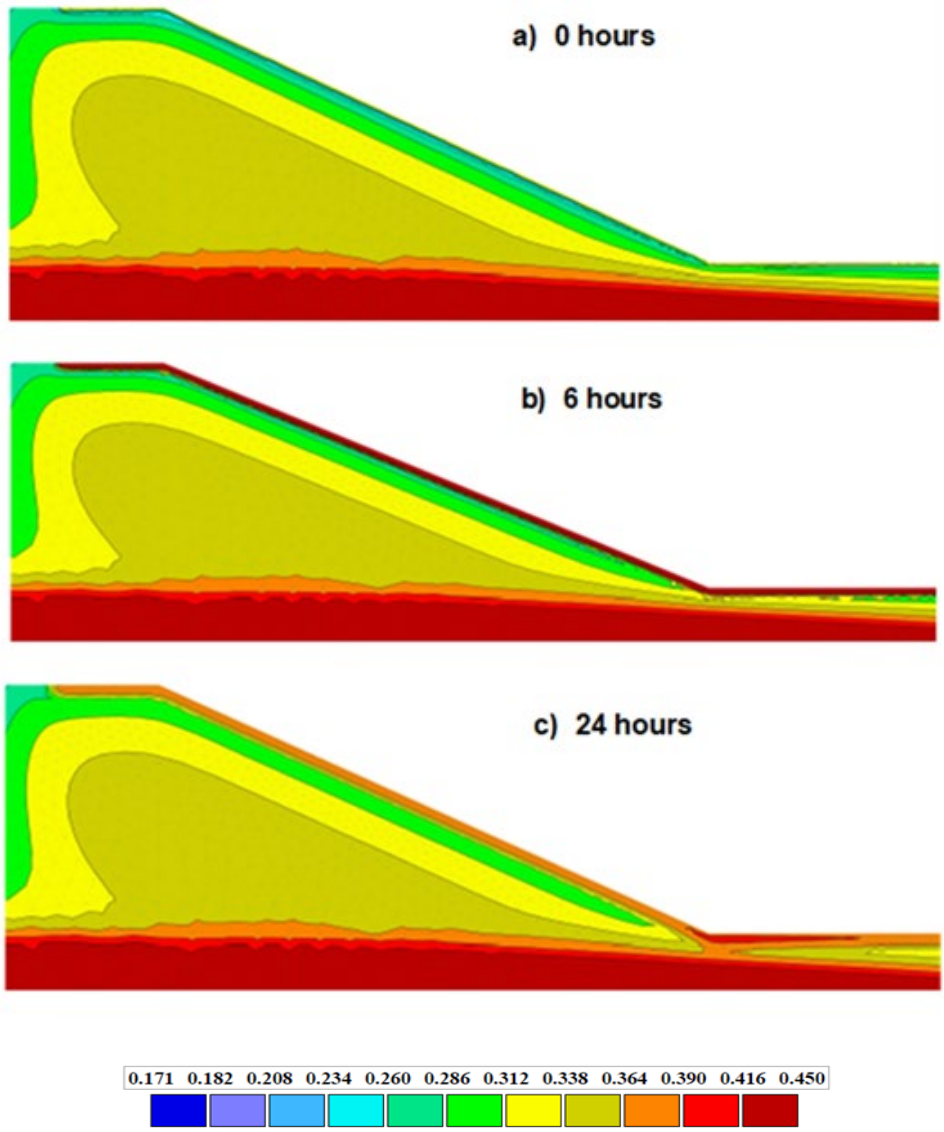

Figure 5.6 Moisture Content -Silt Embankment -Niagara Falls – Fut. IP50% - T50 yrs. Time 0, 6 and 24 hrs

The soil's capacity to retain moisture is also related to particle size, and fine soils, such as silty soils, can retain larger amount of moisture (Leeper et al., 1993). This is evident from that fact that silt has a higher porosity value which means, larger volume of water is required to reach saturation in comparison to sand. Therefore, a thicker saturated region near the surface develops for the sand embankment in comparison to silt embankment.

The comparison of moisture content profiles for sand and silt embankment at 24 hours indicates a larger recovery toward the initial moisture content for sand embankment than for silt embankment (Figure 5.5 (c) and Figure 5.6 (c)). This is also related to the difference in conduction and retention properties of sand and silt materials. Silt has higher retention (more capillarity) and lower conduction resulting in less gravity movement of water than sand over the same time period. In contrast to sand embankment, the slope toe area remains nearly saturated 18 hr after end of precipitation.

5.3.2 Suction Stress Response

In this section, the impact of moisture content distribution on the suction stress within the unsaturated surficial section of sandy and silty embankments is discussed. The evolution of suction stress for sand and silt embankments in Niagara Falls for the extreme precipitation event is illustrated on Figure 5.7 and Figure 5.9. In the sand embankments the suction stress varies from 3.8 kPa to 0 kPa from beginning of the precipitation until the end of the extreme event and then recovers to 2.2 kPa at the end of assessment (i.e., Time 24 hrs).

Figure 5.7 a), b), and c)., specifically show the suction stress at the beginning of precipitation (i.e., Time 0), end of precipitation (i.e., Time 6 hrs) and 24 hours after the commencement of precipitation, respectively. At the Time 0, for initial condition, a suction stress of approximate 3.8 kPa within the top 0.7 m of slope surface can been observed. After the 6 hours, suction stress reduced to 0 kPa, within this region, this is consistent with the moisture content distribution, presented and discussed earlier. It can also be observed that the suction stress after 24 hours, recovers to an approximate value of 2.2 kPa. This can be attributed to the decrease in moisture content from Time 6 hrs (i.e., end of the precipitation) to Time 24 hrs (i.e., end of analysis).

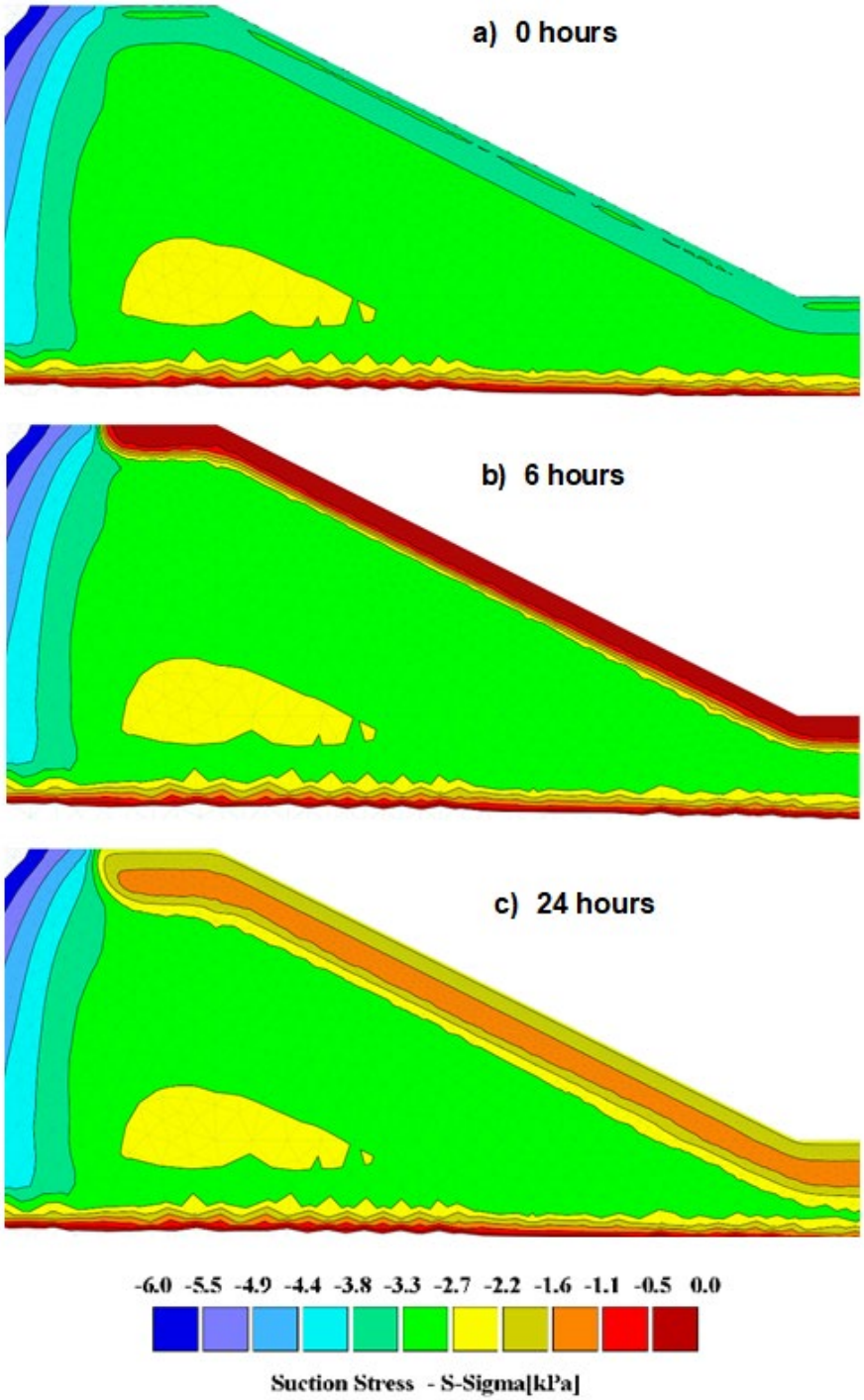

Figure 5.7 Suction Stress - Sand Embankment - Niagara Falls - Fut. IP 50% - T50 yr. Time, 0, 6 and 24 hours

The suction stress distribution for the same climatic conditions for silt embankment is presented on Figure 5.9. Similar to sand embankment, suction profiles are for start, end and 18 hours following the extreme precipitation event. A review of this figure indicates that during the precipitation event the suction stress decreases from 12.7 kPa to 0 kPa in the top portions of the slope area (Figure 5.9 a and b). The depth of this zone is consistent with depth of moisture content increase as discussed earlier. It can also be observed that within this area, the suction stress recovers to 5.5 kPa after the redistribution of moisture content at the Time 24 hrs (Figure 5.9 (c)). That is an indication of increase in moisture content distribution with depth which results in decrease in saturation and increase in suction stress at shallower depth at the end of precipitation event.

The dependency of suction stress variation to the evolution of moisture content distribution can be observed for both the sand and silt embankments, as presented above. In general, the temporal and spatial distribution of suction stress for both sand and silt embankments are consistent with the temporal and spatial distribution of moisture content for these embankments. However, the differences in suction stress distribution between the sand and silt embankment are also a function of differences in suction stress characteristic of these materials. This is in addition to the differences in the soil hydraulic properties for these materials which primarily control the spatial and temporal distribution of the moisture content. Figure 5.8 shows the suction stress characteristic curves (SSCC) for sand and silt materials, considered in this research. The X axis shows the effective saturation, and the Y axis is suction stress for sand and silt in kPa. It can be observed that the silt has larger suction stress than sand at similar values of effective saturation. This is attributed to the finer particle size distribution of silt that results in finer pore size distribution. As can be seen on Figure 5.7 and Figure 5.9, (a) and (c), the sand embankments will

gain approximately 60% and the silt embankments will gain approximately 43% of initial suction stress values, within the surficial depths of the slope, 18 hours after the end of precipitation. This is consistent with the respective redistribution of the moisture for sand and silt as described earlier. It should be noted that in general, the evolution of suction stress is a function of the hydraulic behavior that is influenced by hydraulic parameters such as SWCC and hydraulic conductivity. As disscussed in Section 5.3.1, sand has low retention, therefore, draining starts at lower suction value (AEV) and more significant quntaties of moisture drains over a smaller suction range. Both sand and silt soils have different saturated hydraulic conductivites and pore size distribution. Therefore reduction in hydraulic conductivites will be different over similar suction range for both types of soils. In silt embakments it will take longer for suction stress to recover in comparsion to the sand embankments, where redistribution of moisture occurred more rapidly due to higher conduction.

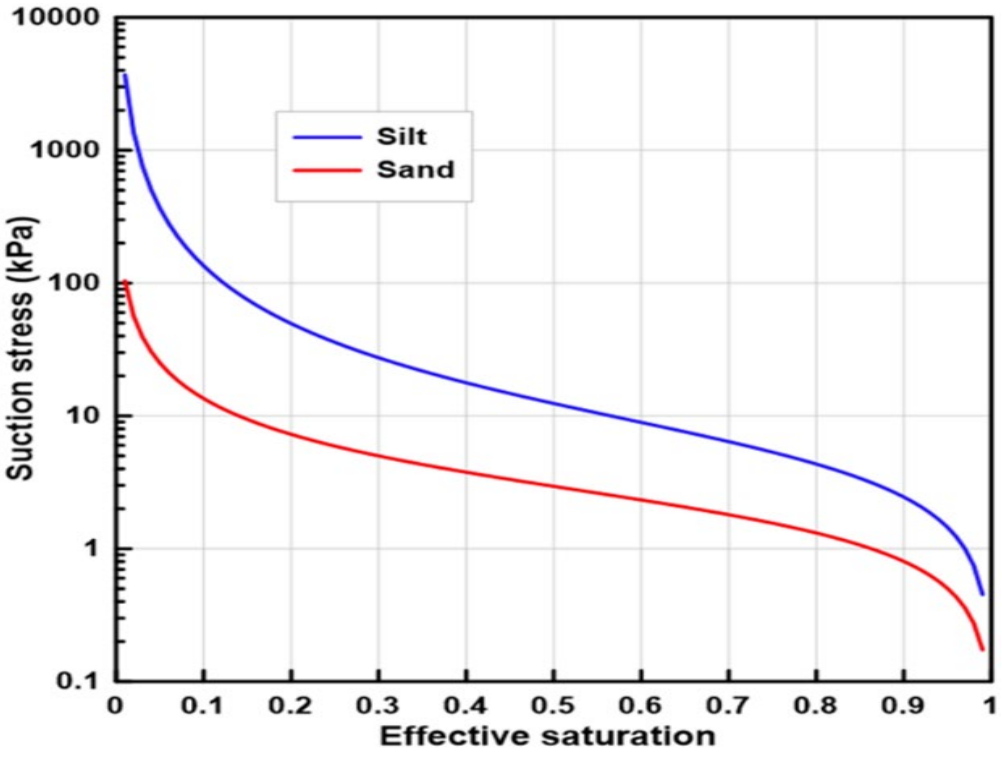

Figure 5.8 Suction Stress vs Effective Saturation - Sand and Silt

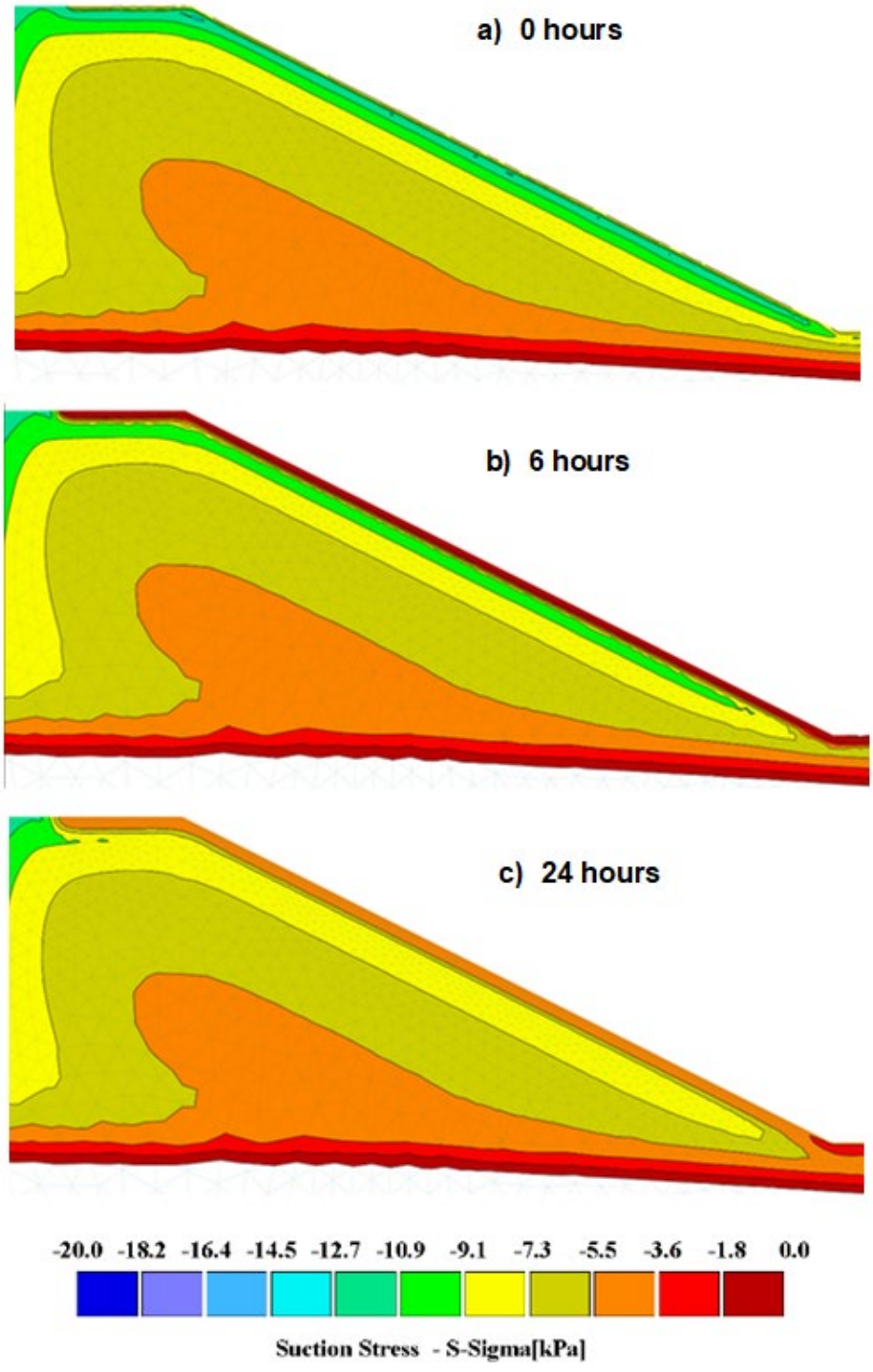

Figure 5.9 Suction Stress – Silt Embankment -Niagara Falls – Fut. IP 50% - T50 yr. Time 0, 6 and 24 hrs.

5.3.3 Field of LFS for Sand and Silt Embankments

In this section the field of LFS for sand and silt embankments in Niagara Falls is presented. Similar to the results presented above these results are for an initial condition of IP 50%, and future storm of six hours with a 50 year return period.

The evolution of A_{LFS}<1.0 and 1.3 for sand and silt embankments, is presented on Figure 5.10 and Figure 5.11, respectively under similar initial and climactic conditions. In silt embankment, increase of A_{LFS}<1 at the toe of slope is observed and 18 hours after the precipitation increased, the different response observed for sand and silt embankments is consistent with hydraulic parameters and shear strength of these two materials, as described in this chapter.

5.4 Changing Climate Impact on Embankments (Field of LFS)

5.4.1 Quantification of LFS Evolution under Changing Climate

Although LFS contour maps provide a general display of slope stability conditions (as demonstrated in Section 5.3.3), a quantitative indicator for LFS is required, particularly when the variation of LFS over time is of interest. Bagheri et al. (2019) defined a slope stability indicator based on the area of LFS (A_{LFS}) corresponding to a particular numerical value for the model cross section, as discussed in the Chapter 4: . For example, the value of A_{LFS}<1 is the area of the zone in which LFS is less than unity. This represents the mass of potential local failure zone in the model domain. This indicator was employed in this study.

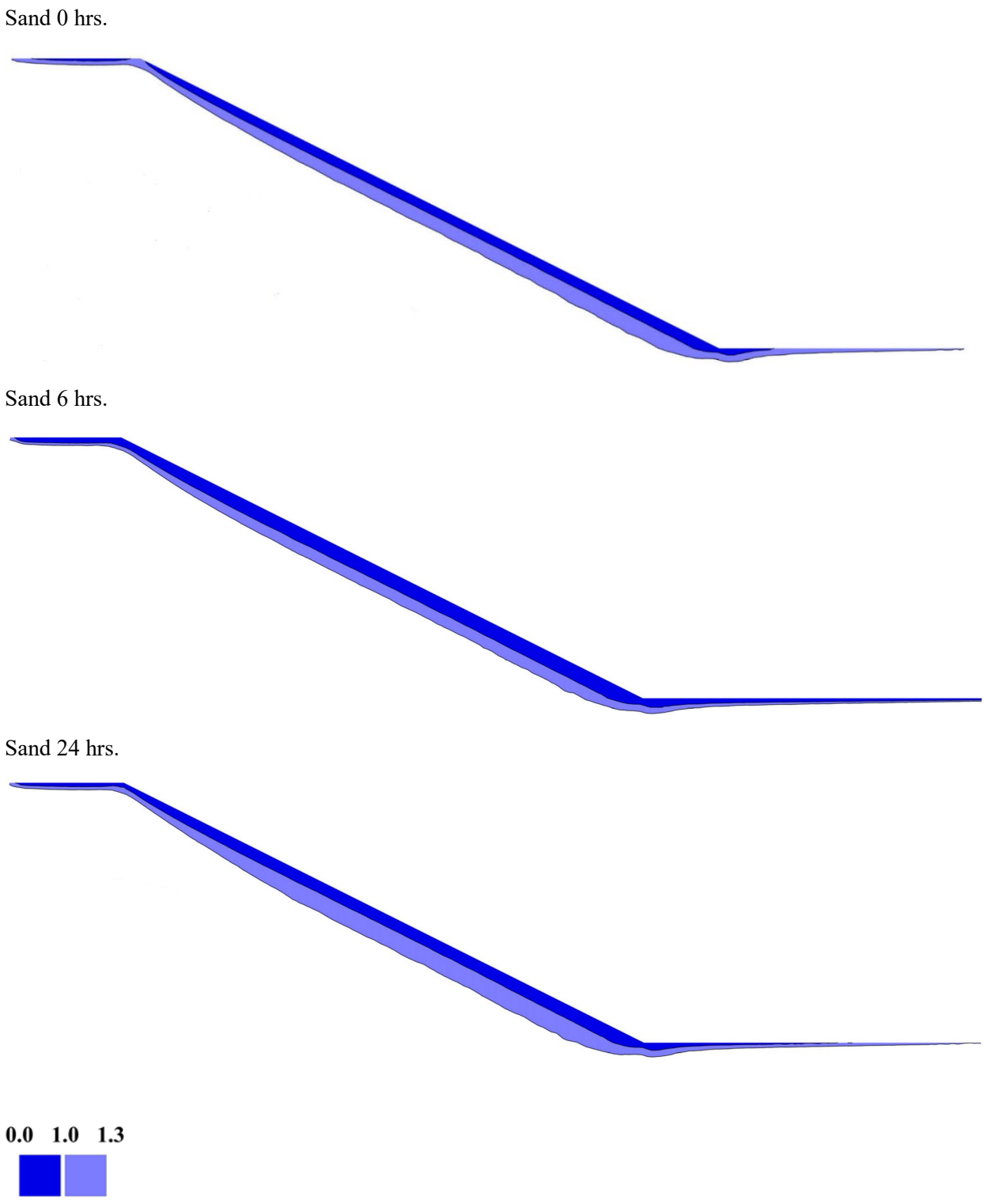

Figure 5.10 Local factor of Safety - Niagara Falls - Sand Embankment - IP 50% - T=50 yr.

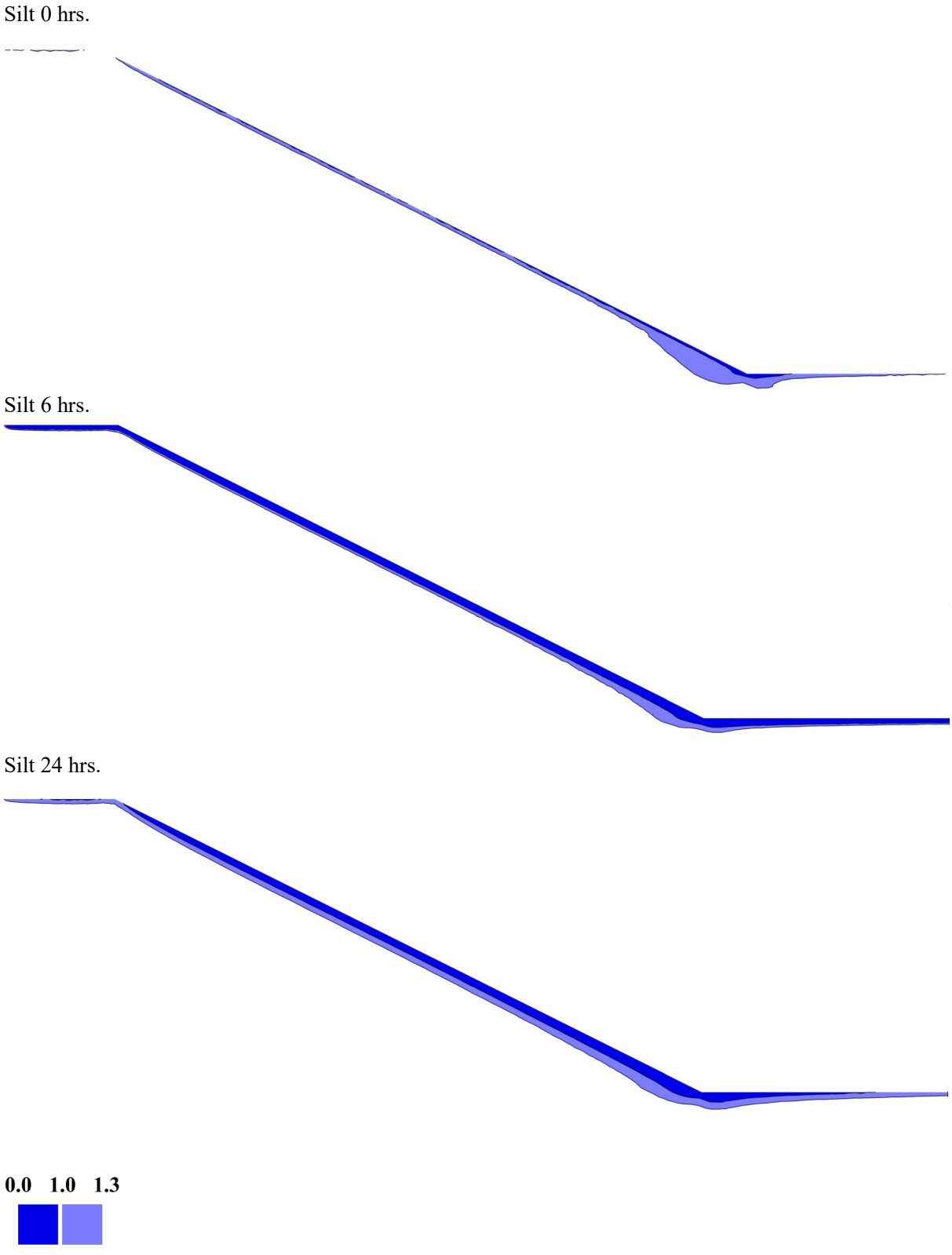

Figure 5.11 Local factor of Safety - Niagara Falls - Silt Embankment - IP 50% - T=50 yr.

Figure 5.12 summarizes the temporal variation of $A_{LFS<1}$ for sand and silt embankments in the City of Niagara Falls. Embankments were assessed for initial conditions corresponding to both IP 50% and IP 90%, as described in Chapter 3: . The results presented on this figure are for historical and future 6-hr extreme precipitation events, for 50 and 100-year return periods. The assessment is carried out for a 24-hour duration, where 18 hours redistribution period is simulated following the 6-hour extreme precipitation events. Moreover, in both sand and silt embankments under IP 90% initial condition, the decrease in $A_{LFS<1}$, from the peak to the end of assessment is more significant comparing to the obtained results under IP 50% condition.

The surficial portion of sandy embankments experiences significant amount of stress change due to infiltration whereas, this stress change extends to several meters in silty slopes. This fact is an important factor in slope instability under the precipitation extreme events due to the expected climate changes. The pore pressure distribution and resultant effective stress field in the studied embankments is transient and swayed by different factors such as intensity and duration of extreme events, the slope geometry, soil hydraulic parameters and initial water content distribution. The $A_{LFS<1}$ results presented on Figure 5.12, indicate that for sand embankments, increase in $A_{LFS<1}$ can be observed approximately one and half hour after the start of the precipitation event. This is in contrast to the results for silt embankments where increase in $A_{LFS<1}$ started immediately after the commencement of rainfall.

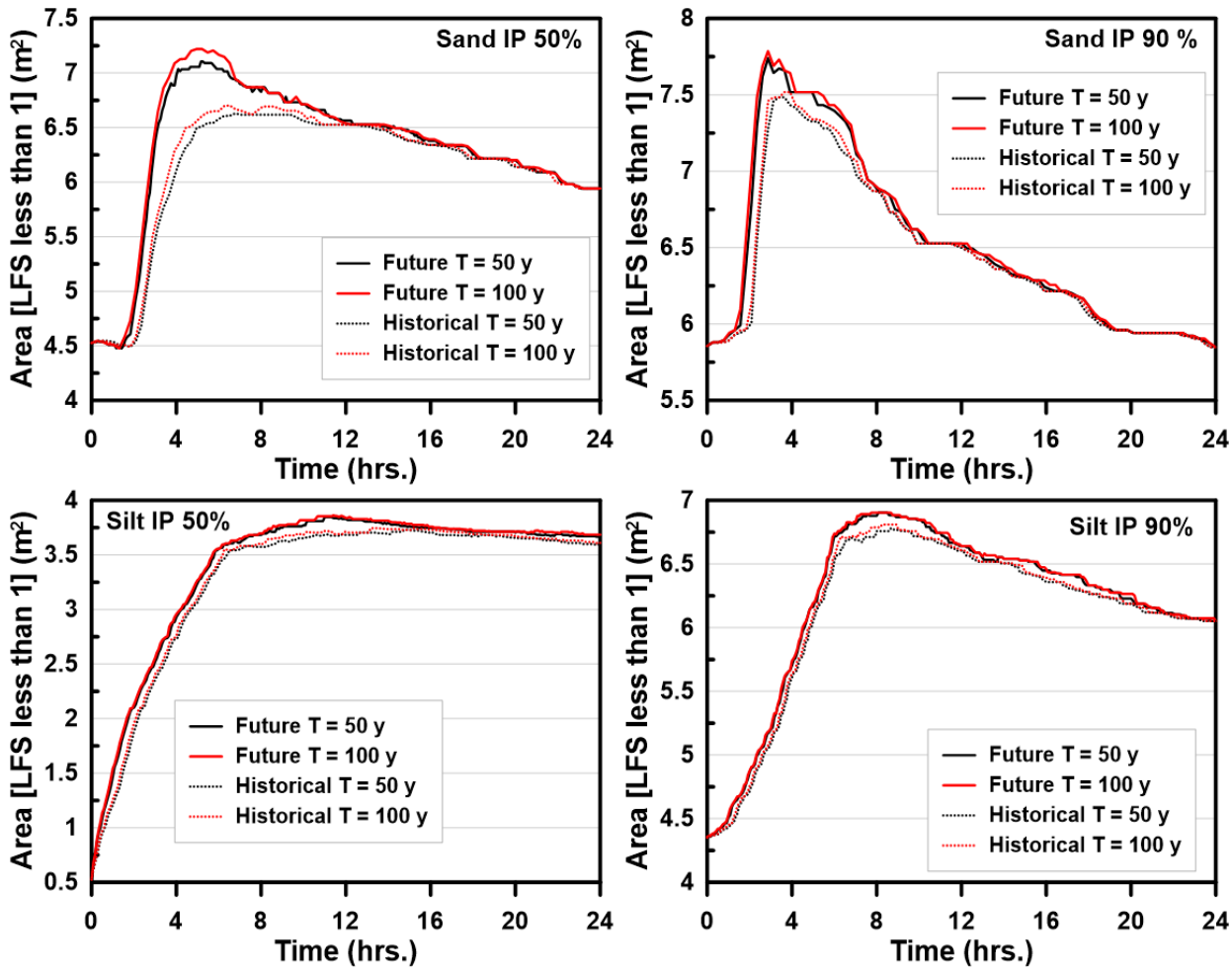

Figure 5.12 Area of LFS <1 (m^2) vs Precipitation time (6 hours) and assessment time (24 hours) Niagara Falls Sand and Silt Embankment – Initial Condition IP 50% and 90%

The above noted differences are related to difference in soil hydraulic properties as well as the dissimilar initial degree of saturations for sand and silt embankments. It should be noted that in this study, the silt embankments were at higher initial degree of saturation in comparison to the sand embankments. It can be seen that for the sand embankments, majority of $A_{LFS<1}$ increase, occurs within 1.5 to 4 hours of the start of precipitation event. In contrast, silt embankment shows immediate but more gradual increases in the development of $A_{LFS<1}$ zone. The immediate increase in $A_{LFS<1}$ for silt embankments is related to the higher initial degree of saturation in comparison to sand embankment. Similarly, more gradual increase is related to lower conduction and higher

retention of silt in comparison to sand, which results in lower infiltration and slower water migration within the embankment.

In terms of climate change all results are indicative of more extensive potential instabilities in the future. This is in line with the climate change predictions as more intense weather events are expected in the future. The results indicate potentially larger increase in areas of instability for sand embankments as opposed to silt embankments. In fact, the increase in areas of instability due to changes in extreme precipitation events appear to be quite modest for silt embankments. This might seem surprising as more drainable materials are generally considered to perform better for embankment construction. However, these results are consistent with results from others. Pk et al. (2018) and Baninajarian (2020), who have reported that the sand embankments are more prone to instabilities for shorter duration, higher intensity precipitation events, while silt embankments are more prone to instabilities under longer duration, lower intensity precipitation events. This is related to the lower hydraulic conductivity of silt materials, where longer duration, lower intensity precipitation events result in larger infiltration as opposed to shorter duration, higher precipitation events which generate more runoff. Since, in the current research the evaluation is for extreme precipitation events, therefore the results are consistent with those reported by Pk et al. (2018) and Baninajarian (2020).

5.5 Effect of Storm Distribution on LFS Results

As described in section 3.3, actual storm distributions for historical extreme events are rarely available and no methods for estimation for such distribution of future events has been reported in the literature. In this research the use of Chicago method for distribution of historical and future extreme events is proposed and implemented. Previous studies by others (Robinson et al. 2017, Pk

et al. 2018) have used storms of constant intensity. In order to quantify the effect of storm distribution on LFS results additional simulations were carried out. These simulations were carried out for sand and silt embankments in the City of Niagara Falls. The initial condition for these simulations were of IP 50% and historical extreme events with 50-year return periods were considered. The intensity over the six-hour extreme events was considered to be constant. Figure 5.13. and Figure 5.14 compare the temporal distribution of A_{LFS} <1 for storms with constant and variable intensity for sand and silt embankments respectively. Results indicate that assumption of constant intensity extreme events results in slightly higher estimates of A_{LFS} <1. The difference between the constant intensity and Chicago storms are more pronounced for silt embankment. Therefore, it can be concluded that the assumption of constant intensity storms results in more conservative estimates of A_{LFS} <1.

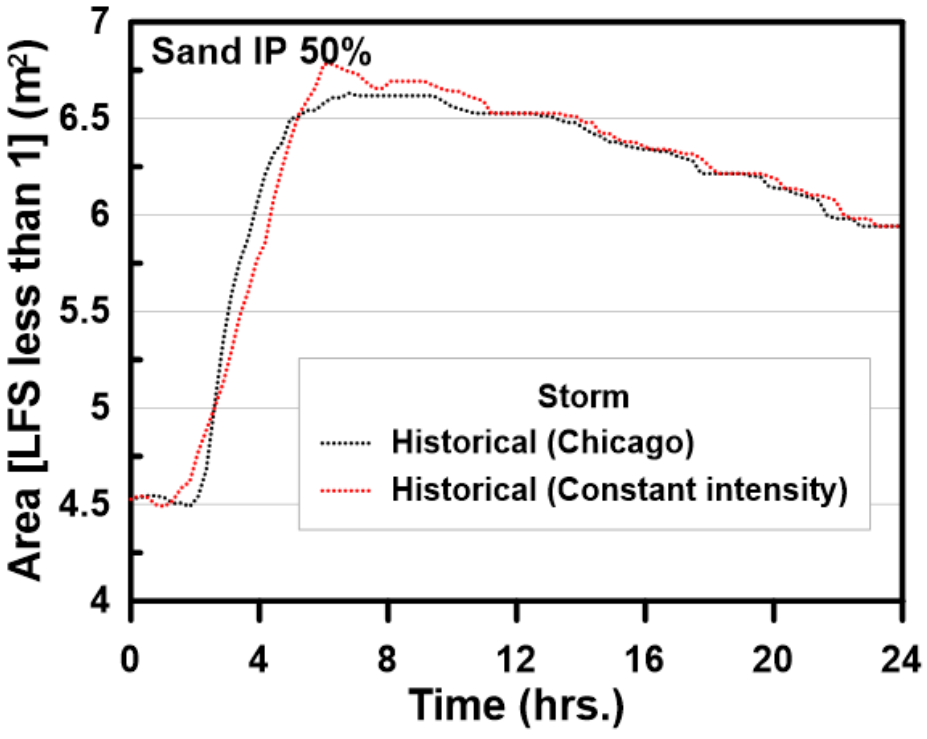

Figure 5.13 Comparison of A_{LFS} <1 for Sand Embankment for Storms of Constant and Variable Intensity

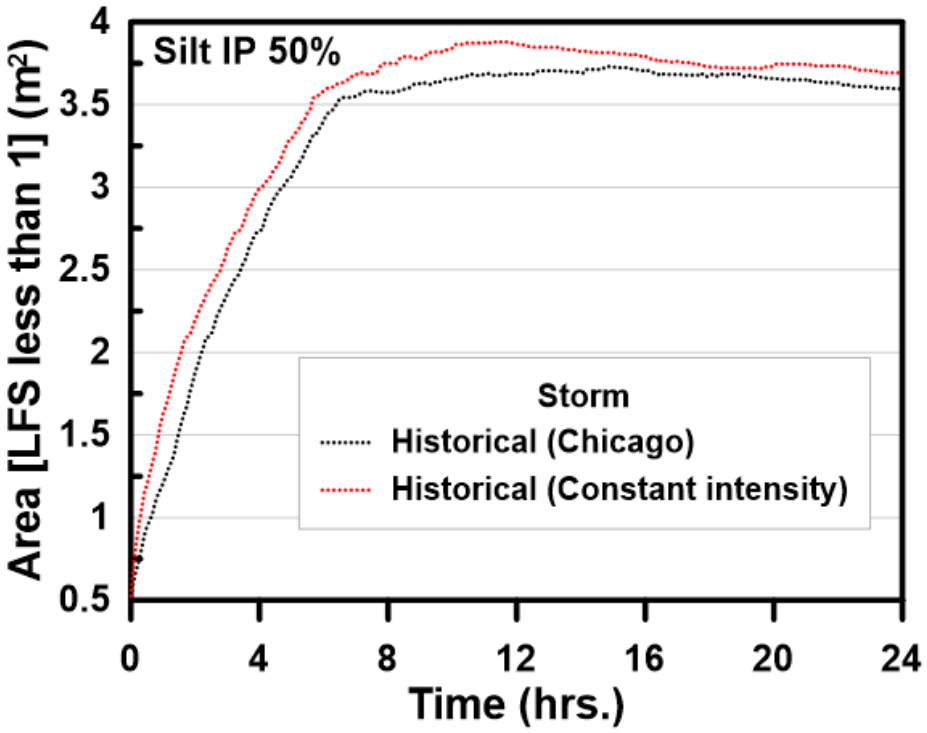

Figure 5.14 Comparison of A_{LFS} <1 for Silt Embankment for Storms of Constant and Variable Intensity

5.6 Comparison of A_{LFS}<1 for the Cities of Niagara Falls, London, and Ottawa

In this section the effect of climate change on embankments in the cities of Niagara Falls, London and Ottawa is compared. This comparison is presented in the form of percentage increase in A_{LFS}<1 in the future relative to the historical conditions. In total forty-eight simulations for the cities of Niagara Falls, London and Ottawa were carried out. The embankment geometry was same for all these simulations. Soil hydraulic and geotechnical properties were representative of sand and silt materials as described earlier. For each city, simulations were carried out for IP 50% and IP 90% initial conditions for the historical and future periods as described in section 4.4. Similarly, for each city, historical and future extreme precipitation events with 50- and 100-year return periods as described in section 3.3 and Appendix A were used.

Figure 5.15 and Figure 5.16 present the comparison for sand and silt embankments respectively. From the results it can be expected that the area of embankment with LFS < 1will increase in the future. An increase can be expected for all the three cities considered in this research, irrespective of the initial conditions and return period of the extreme events. These increases observed approximately 3 hours and 9 hours after beginning of the extreme events for sand and silt embankments, respectively and ranged from 1.4% to approximately 8 %. For sand embankments, with one exception, extreme precipitation events with 100-year return period generally result in higher increases in A_{LFS}< 1 in the future. Surprisingly, lowest increase in A_{LFS}< 1 can be observed for silt embankments in the City of Niagara Falls, although percentage change in the future intensity (Figure 3.4) is expected to be larger than the cities of London and Ottawa. This might be counter intuitive, however, as also mentioned earlier, that owing to lower conductivity of the silt material, larger increases in precipitation intensities can potentially result in larger quantities of runoff with minimal increases in infiltration. Similar observations have been made by Pk et al. (2018).

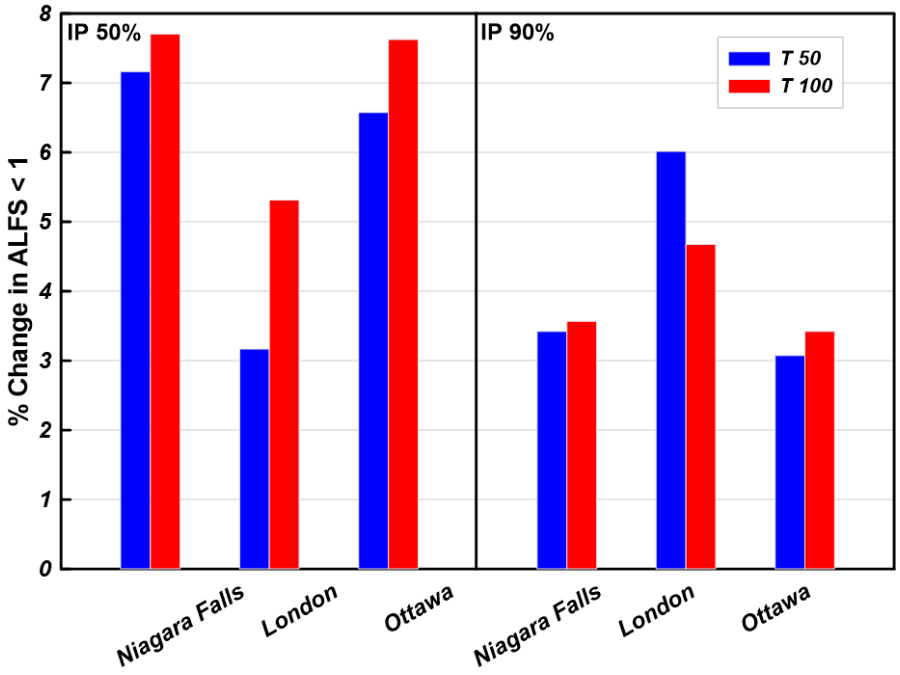

Figure 5.15 LFS Comparison Chart - Sand

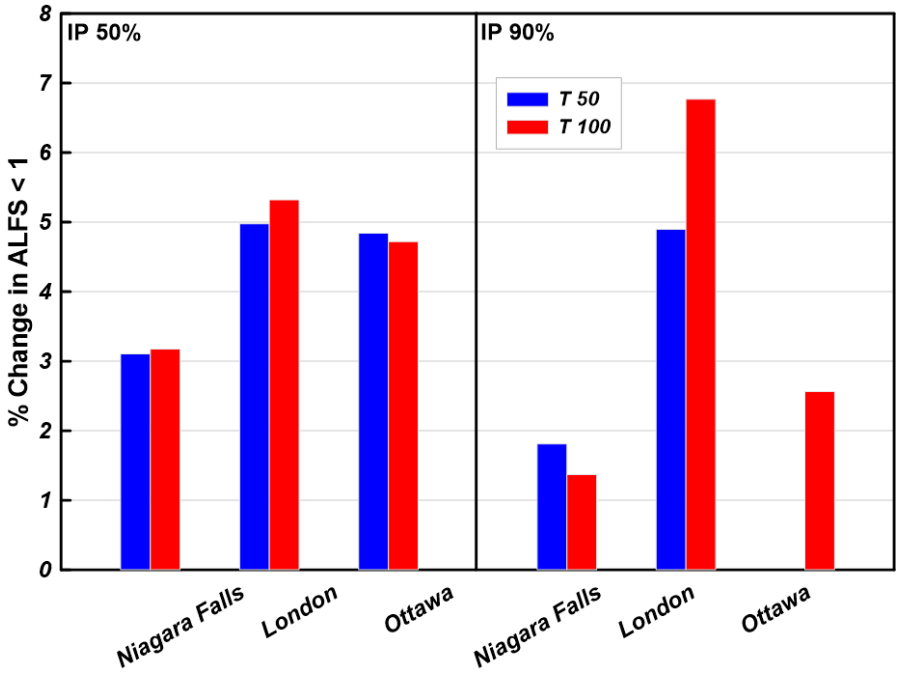

Figure 5.16-LFS Comparison Chart – Silt

Chapter 6: Summary, Conclusions, and Recommendations for Future Research

6.1 Conclusions

In this study, the effect of climate change on the stability of typical, sand and silt embankments, in cities of Niagara Falls, London and Ottawa are investigated in changing climate. The assessment is done by estimating the field of local factor of safety. A variably saturated seepage model equipped with soil-atmosphere boundary condition was employed to calculate the soil moisture distribution within the embankments. The effect of water content variation on the in-situ effective stress field was taken into consideration using the suction stress state concept within the unsaturated soil mechanics framework.

In the method employed, the in-situ stress field is calculated based on an elastic finite element analysis employing the concept of Local Factor of safety (LFS). The area of zone in which LFS is less than unity ($A_{LFS}<1$) was considered as the indicator of the potential failure mass. The contour of LFS<1 was compared with yield points obtained from an elasto-plastic finite element analysis. The comparison is also made with both the conventional and finite element limit equilibrium methods. The variation of $A_{LFS}<1$ over time is investigated for silt and sand embankments subjected to historical and future, 6-hr extreme precipitation events.

Results of the assessments are presented in the form of temporal variation of $A_{LFS}<1$ over the course of extreme precipitation events and 18 hours following the extreme event. Results for future extreme events are compared with those for historical events. Relative differences in climate change effects on slope stability, among the cities of Niagara Falls, Ottawa and London are also presented.

6.2 Research Contribution

The research carried out in this thesis, presents the first study to quantify the effect of climate change on the stability of highway embankments using the concept of Local Factor of Safety (LFS). This is also the first study to provide a systematic comparison of LFS approach to other well-established methods such as finite element limit equilibrium method and finite element analyses using an elasto-plastic model. The finding of this research has been presented in Canadian geotechnical annual conferences and are published in the conference proceeding as follows:

1. Bagheri F., Ghassemi A. and Bashir R. (2019). Assessment of the Effects of Climate Change on Slope Stability using Local Factor of Safety, 72nd Canadian Geotechnical Society Annual Conference, St. John's, Newfoundland, Canada.

2. Bagheri F., Ghassemi A. and Bashir R. (2020). Assessment of Local Factor of Safety Field for Variably Saturated Embankments due to Climate Change Using In-Situ Stress Finite Element Analysis, 73rd Canadian Geotechnical Society Annual Conference, GeoVirtual, Canada.

6.3 Recommendations for Future Research

As described in this thesis, priority in the current engineering assessments was to check the feasibility of LFS approach in quantifying the effect of climate change on the stability of embankment slopes for select locations in the province of Ontario. The Cube module of Hydrus 2D/3D used for the current research is not capable of carrying out deformation assessments within the unsaturated soil mechanics framework. In this research, the LFS analysis carried out using HYDRUS (2D/3D) program version 3.01.1360. A new version of Cube (version 3.04) has been released in May 2021 and is now capable of carrying out deformation assessments within the unsaturated soil mechanics framework. It is recommended that the deformation assessments for

embankments slopes should be considered for future studies. It is also recommended that the similar evaluations should be carried out for other cities in the province of Ontario. It is also recommended that extreme precipitations events of different durations should be considered in future assessments. The soil parameters considered in this research are for typical sand and silt materials used in embankment construction in the province of Ontario. It is recommended that the variability in hydraulic and geotechnical parameters should be considered within a probabilistic framework.

References

Adem, H. and Vanapalli, S. 2014. Soil–environment Interactions Modelling for Expansive Soils, Environmental Geotechnics, 3(3): 178-187.

Arairo W., Prunier F., Djeran-Maigre I. and Millard A. 2015. Three-Dimensional Analysis of Hydraulic Effect on Unsaturated Slope Stability, Environmental Geotechnics 3(1): 36–46.

Bagheri F., Ghassemi A. and Bashir R. 2019. Assessment of the Effects of Climate Change on Slope Stability using Local Factor of Safety, 72nd Canadian Geotechnical Society Annual Conference, St. John's, Newfoundland, Canada.

Bagheri F., Ghassemi A. and Bashir R. 2020. Assessment of Local Factor of Safety Field for Variably Saturated Embankments due to Climate Change Using In-Situ Stress Finite Element Analysis, 73rd Canadian Geotechnical Society Annual Conference, GeoVirtual, Canada.

Baninajarian L. 2020, Effect of Future Extreme Precipitation Events on the Stability of Soil Embankments Across Ontario, MASc. Thesis, York University, Toronto, Ontario, Canada.

Bashir R., Ghassemi A., Baninajarian L., Moustafa M. 2021. Effect of Climate Change on Embankment Stability, Ministry of Transportation Ontario, Highway Infrastructure and Innovation Funding Program (HIIFP).

Bishop, A. W. and Blight, G. E., 1963. Some Aspects of Effective Stress in Saturated and Unsaturated Soils. Geotechnique, 13: 177-197.

Bishop, A.W. 1959. The Principle of Effective Stress. Teknisk Ukeblad, 39: 859–863.

Bishop, C. 1954. Coden versus Sigils. Journal of the American Society for Information Science, 5(1): 28.

Batali, L. and Andreea, C., 2016. Slope Stability Analysis Using the Unsaturated Stress Analysis. Case Study. Procedia Engineering, 143, pp.284-291.

Brown, T. J., Hall, B. L., & Westerling, A. L. 2004. The impact of twenty-first century climate change on wildland fire danger in the western United States: an applications perspective. Climatic change, 62(1), 365-388.

Coe, J. and Godt, W. 2012. Review of approaches for assessing the impact of climate change on landslide hazards, CRC Press, ISBN 9780415621236

CCCR. 2019. Canada's Changing Climate Report available from https://changingclimate.ca/CCCR2019/

CCDP. 2018. Ontario Climate Change Data Portal. Available from http://www.ontarioccdp.ca.

Ciabatta, L., Camici, S., Brocca, L., Ponziani, F., Stelluti, M., Berni, N., & Moramarco, T. J. J. O. H. 2016. Assessing the impact of climate-change scenarios on landslide occurrence in Umbria Region, Italy. Journal of Hydrology, 541, 285-295.

Coleman, J. D. 1962. Stress-strain Relations for Partly Saturated Soil. Geotechnique, 12(4): 348-350.

Collison, A., Wade, S., Griffiths, J. and Dehn, M. 2000. Modelling The Impact of Predicted Climate Change on Landslide Frequency and Magnitude in SE England. Engineering Geology, 55(3): 205–218.

Dikau, R., & Schrott, L. 1999. The temporal stability and activity of landslides in Europe with respect to climatic change (TESLEC): main objectives and results. Geomorphology, 30(1-2), 1-12.

Dixon, N. and Brook, E., 2007. Impact of predicted climate change on landslide reactivation: case study of Mam Tor, UK. Landslides, 4(2), pp.137-147.

Duncan, J. M., & Wright, S. G. 1980. The accuracy of equilibrium methods of slope stability analysis. Engineering geology, 16(1-2), 5-17.

Environment and Climate Change Canada. 2018. Historical Climate Data - Environment and Climate Change Canada. Available from https://climate.weather.gc.ca/historical_data/search_historic_data_e.html.

Fallah-Ghalhari, G., Shakeri, F. and Dadashi-Roudbari, A., 2019. Impacts of climate changes on the maximum and minimum temperature in Iran. Theoretical and Applied Climatology, 138(3-4), pp.1539-1562.

Fellenius, W.,1936. Calculation of the Stability of Earth Dams, Trans. 2nd Cong. on Large Dams, Vol 4, p 445

Fredlund, D. G. and Morgenstern, N. R. 1977. Stress State Variables for Unsaturated Soils. Journal of Geotechnical and Geoenvironmental Engineering, American Society of Civil Engineering, 103(5): 447–466.

Fredlund, D.G., Rahardjo, H. and Fredlund, M.D. 2012. Unsaturated Soil Mechanics in Engineering Practice. Wiley, Hoboken, NJ, USA.

Fredlund, D. G., & Scoular, R. E. G. 1999. Using limit equilibrium concepts in finite element slope stability analysis. In Int. Symp. on Slope Stability Engineering, Matsuyama, Shikoku, Japan (pp. 31-47).

Fredlund, D.G., and Xing, A. 1994. Equations for the soil-water characteristic curve. In Canadian Geotechnical Journal.

Gariano, S. L., & Guzzetti, F. 2016. Landslides in a changing climate. Earth-Science Reviews, 162, 227-252.

Geo-slope International Ltd. 2016 . Stability Modeling with SLOPE/W: An Engineering Methodology (Computer Program). GEOSLOPE/W International Ltd., Calgary, Alberta, Canada.

Griffiths, D. V., & Fenton, G. A. 2004. Probabilistic slope stability analysis by finite elements. Journal of geotechnical and geoenvironmental engineering, 130(5), 507-518.

Hershfield, D. M. 1979. Freeze-thaw cycles, potholes, and the winter of 1977–78. Journal of Applied Meteorology, 18, 1003–1007.

Ho, E., & Gough, W. A. 2006. Freeze thaw cycles in Toronto, Canada in a changing climate. Theoretical and Applied Climatology, 83, 203–210. doi:10.1007/s00704-005-0167-7

IPCC. 2013. Summary of IPCC, 2013. Summary for Policymakers. Climate Change 2013. The Physical Science Basis. Contribution of Working Group I to the Fifth Assessment Report of the Intergovernmental Panel on Climate Change [Stocker, T.F., D. Qin, G.-K. Plattner, M. Tignor, S.K. Allen, J. Boschung, A. Nauels, Y. Xia, V. Bex and P.M. Midgley (eds.)]. Cambridge University Press, Cambridge, United Kingdom and New York, NY, USA.

IPCC 2014: Climate Change 2014: Synthesis Report. Contribution of Working Groups I, II and III to the Fifth Assessment Report of the Intergovernmental Panel on Climate Change [Core Writing Team, R.K. Pachauri and L.A. Meyer (eds.)]. IPCC, Geneva, Switzerland, 151 pp.

Janbu, N. 1973. Slope stability computations. Publication of: Wiley (John) and Sons, Incorporated.

Keifer, C.J. and Chu, H.H. 1957. Synthetic Storm Pattern for Drainage Design. Journal of the Hydraulics Division, 83(4): 1–25.

Krahn, J. 2003. The 2001 RM Hardy Lecture: The limits of limit equilibrium analyses. Canadian Geotechnical Journal, 40(3), 643-660.

Kwak, J., Kim, S., Singh, V. P., Kim, H. S., Kim, D., Hong, S., & Lee, K. 2015. Impact of climate change on hydrological droughts in the upper Namhan River basin, Korea. KSCE Journal of Civil Engineering, 19(2), 376-384.

Labajo, A. L., Egido, M., Martín, Q., Labajo, J., & Labajo, J. L. 2014. Definition and temporal evolution of the heat and cold waves over the Spanish Central Plateau from 1961 to 2010. Atmósfera, 27(3), 273-286.

Lee, S. R., Kim, Y. K., Kwon, H. S., & Hwang, D. 2009. An alternative slope design methodology to prevent slope failures due to rainfall infiltration. In Proceedings of the 17th International Conference on Soil Mechanics and Geotechnical Engineering (Volumes 1, 2, 3 and 4) (pp. 1694-1697). IOS Press.

Liu, S., Su, Z., Li, M., & Shao, L. 2020. Slope stability analysis using elastic finite element stress fields. Engineering Geology, 105673.

López-Díaz, F., Conde, C., & Sánchez, O. 2013. Analysis of indices of extreme temperature events at Apizaco, Tlaxcala, Mexico: 1952-2003. Atmósfera, 26(3), 349-358.

Lu, N., Godt, J. W., & Wu, D. T. 2010. A closed-form equation for effective stress in unsaturated soil. Water Resources Research, 46(5).

Lu, N., & Godt, J. W. 2013. Hillslope hydrology and stability. Cambridge University Press.

Lu, N., & Kaya, M. 2013. A drying cake method for measuring suction-stress characteristic curve, soil–water-retention curve, and hydraulic conductivity function. Geotechnical Testing Journal, 36(1), 1-19.

Lu, N., and Likos, W.J. 2006. Suction Stress Characteristic Curve for Unsaturated Soil. Journal of Geotechnical and Geoenvironmental Engineering, 132(2): 131–142.

Lu, N., Şener-Kaya, B., Wayllace, A., & Godt, J. W. 2012. Analysis of rainfall-induced slope instability using a field of local factor of safety. Water Resources Research, 48(9).

Lu, N., Wayllace, A., & Formetta, G. 2016. The Slope Cube Module. Soil Water Retention, LLC: Madison, WI, USA.

Marsalek, J., & Watt, W. E. 1984. Design storms for urban drainage design. Canadian Journal of Civil Engineering, 11(3), 574-584.

Morgenstern, N.R. and Price, V.E. 1965. The Analysis of the Stability of General Slip Surface. Geotechnique 15(1): 79-93.

MTO. 1997. Drainage Management Manual. Ronin House Publishing, under contract from Ministry of Transportation of Ontario, Ottawa, Ontario, Canada.

MTO. 2018. (Ministry of Transportation), IDF Curve Look-up. Ministry of Transportation, Toronto, ON, Canada.

Mualem, Y. 1976. A New Model for Predicting The Hydraulic Conductivity of Unsaturated Porous Media. Water Resources Research, 12(3): 513–522.

Pk, S. 2017. Effects of Climate Change on Soil Embankments, MSc Thesis, York University.

Pk, S., Bashir, R., and Beddoe, R. 2018. Effect of Climate Change on Earthen Embankments in Southern Ontario, Canada. Environmental Geotechnics: 1–70.

Prodanovic, P., & Simonovic, S. P. 2004. Generation of synthetic design storms for the Upper Thames River basin. Department of Civil and Environmental Engineering, The University of Western Ontario.

Rahardjo, H., Nio, A.S., Leong, E.C., and Song, N.Y. 2010. Effects of Groundwater Table Position and Soil Properties on Stability of Slope during Rainfall. Journal of Geotechnical and Geoenvironmental Engineering, 136(11): 1555–1564.

Rianna, G., Pagano, L., & Urciuoli, G. 2014. Rainfall patterns triggering shallow flowslides in pyroclastic soils. Engineering Geology, 174, 22-35.

Robinson, J.D., Vahedifard, F., and AghaKouchak, A. 2017. Rainfall-triggered slope instabilities under a changing climate: comparative study using historical and projected precipitation extremes. Canadian Geotechnical Journal, 54(1): 117–127.

Rockel, B., & Geyer, B. 2008. The performance of the regional climate model CLM in different climate regions, based on the example of precipitation. Meteorologische Zeitschrift, 17(4), 487-498.

Rouainia, M., Davies, O., O'Brien, T., and Glendinning, S. 2009. Numerical modelling of climate effects on slope stability. Proceedings of the Institution of Civil Engineers - Engineering Sustainability, 162(2): 81–89.

Schmidlin, T. W., Derthier, B. E., & Eggleston, K. L. 1987. Freeze-thawdays in the northeastern United States. Journal of Climate and Applied Meteorology, 26, 142–155.

Schmidt, J., & Dikau, R. 2004. Modeling historical climate variability and slope stability. Geomorphology, 60(3-4), 433-447.

Scripca, A. S., Strapazan, C., & Holobâca, I. H. 2016. Regional aspects of the variability of atmospheric precipitations in winter and summer seasons in Europe during 2001-2090. Aerul si Apa. Componente ale Mediului, (2016): 143-150.

Šimŭnek, J., Van Genuchten, M.T., and Šejna, M. 2006. The HYDRUS software package for simulating two-and Three-Dimensional Movement of Water, Heat, and Multiple Solutes in Variably Saturated Media. Technical manual, version 1: 241.

Strauch, A.M., MacKenzie, R.A., Giardina, C.P., Bruland, G.L. 2015. Climate driven changes to rainfall and streamflow patterns in a model tropical island hydrological system. Journal of Hydrology, 523, 160-169.

Taban, A., Sadeghi, M. M., & Rowshanzamir, M. A. (2018). Estimation of van Genuchten SWCC model for unsaturated sands by means of the genetic programming. Scientia Iranica, 25(4), 2026-2038.

Tao, H., Gemmer, M., Jiang, J., Lai, X., & Zhang, Z. 2012. Assessment of CMIP3 climate models and projected changes of precipitation and temperature in the Yangtze River Basin, China. Climatic change, 111(3), 737-751.

Thornthwaite, C., 1948. An Approach Toward a Rational Classification of Climate. Soil Science, 66(1), p.77.

Thornthwaite, C. and Hare, F. K. 1955. La clasificación climatológica en dasonomía. Unasylva, 9(2), 53-103.

Taylor, K. E., Stouffer, R. J., & Meehl, G. A. 2012. An overview of CMIP5 and the experiment design. Bulletin of the American meteorological Society, 93(4), 485-498.

USACE. 1984. Hydrologic Modeling System HEC-HMS Technical Reference Manual CPD-74B.

USDA. 2018. National Soil Survey Handbook (NSSH) | NRCS Soils. https://www.nrcs.usda.gov/wps/portal/nrcs/detail/soils/ref/?cid=nrcs142p2_054242.

van Genuchten, M.Th. 1980. A Closed Form Equation for Predicting the Hydraulic Conductivity of Unsaturated Soils. 44: 892–898.

Vanapalli, S. K., Fredlund, D. G., Pufahl, D. E., & Clifton, A. W. 1996. Model for the prediction of shear strength with respect to soil suction. Canadian geotechnical journal, 33(3), 379-392.

Veneziano, D., & Villani, P. 1999. Best linear unbiased design hyetograph. Water Resources Research, 35(9), 2725-2738.

Vincent, L.A. Zhang, X., . Mekis, É, . Wan, H & Bush, E.J. (2018) Changes in Canada's Climate: Trends in Indices Based on Daily Temperature and Precipitation Data, Atmosphere-Ocean, 56:5, 332-349, DOI: 10.1080/07055900.2018.1514579

Watt, W. E., Chow, K. C. A., Hogg, W. D., & Lathem, K. W. 1986. A 1-h urban design storm for Canada. Canadian Journal of Civil Engineering, 13(3), 293-300.

Yeh, H. and Tsai, Y., 2018. Effect of Variations in Long-Duration Rainfall Intensity on Unsaturated Slope Stability. Water, 10(4), p.479.

Yen, B. and Chow, V., 1980. Design Hyetographs for Small Drainage Structures. Journal of the Hydraulics Division, 106(6), pp.1055-1076.

Zhang, X., Flato, G., Kirchmeier-Young, M., Vincent, L., Wan, H., Wang, X., Rong, R., Fyfe, J., Li, G., Kharin, V.V. 2019: Changes in Temperature and Precipitation Across Canada; Chapter 4 in Bush, E. and Lemmen, D.S. (Eds.) Canada's Changing Climate Report. Government of Canada, Ottawa, Ontario, pp 112-193.

Appendices

Appendix A: IDF Curves

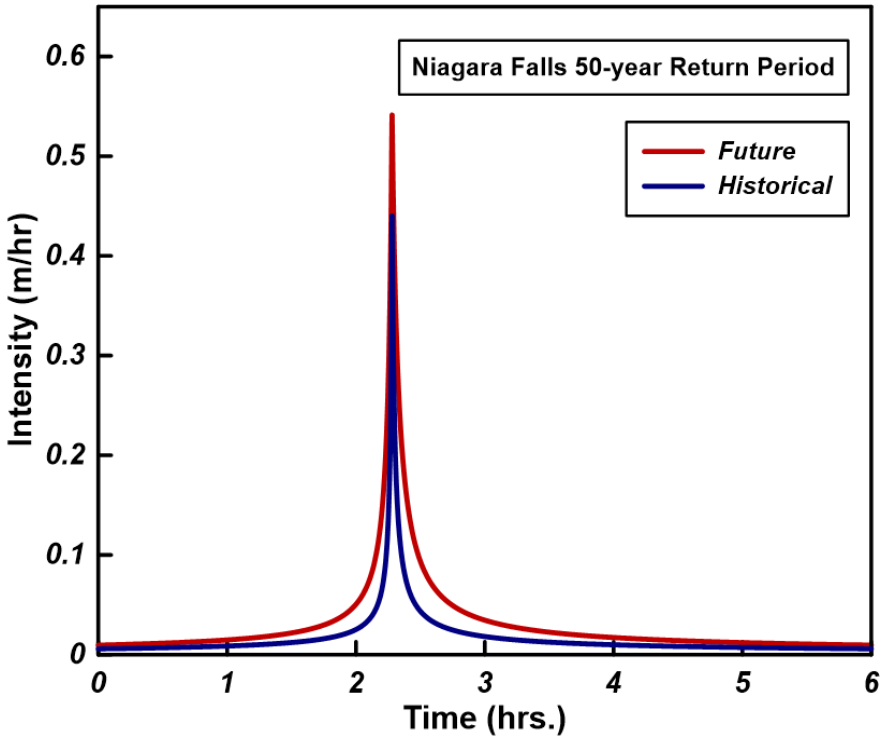

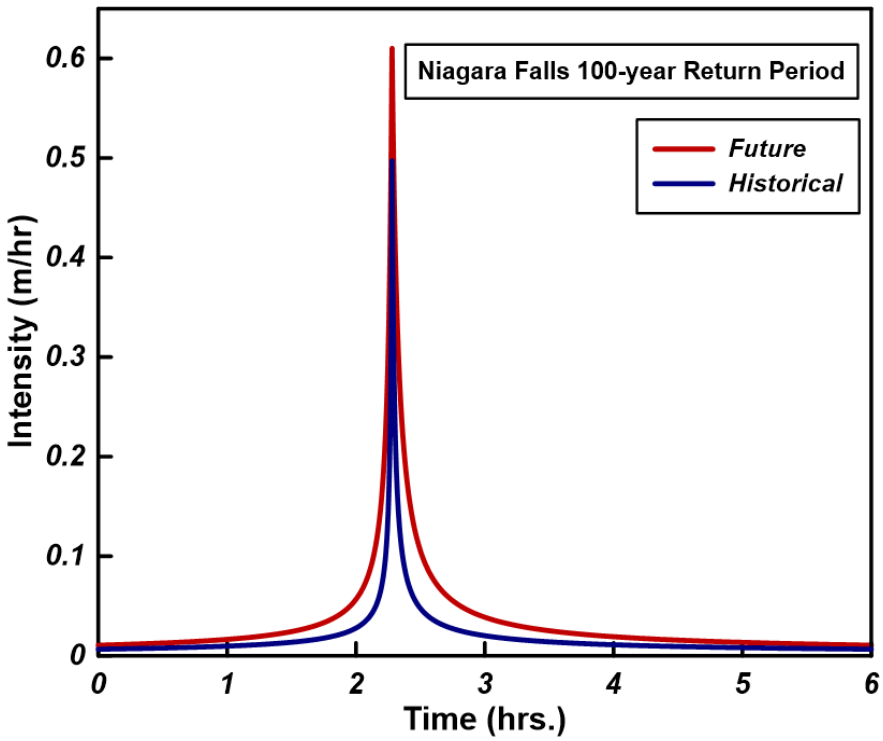

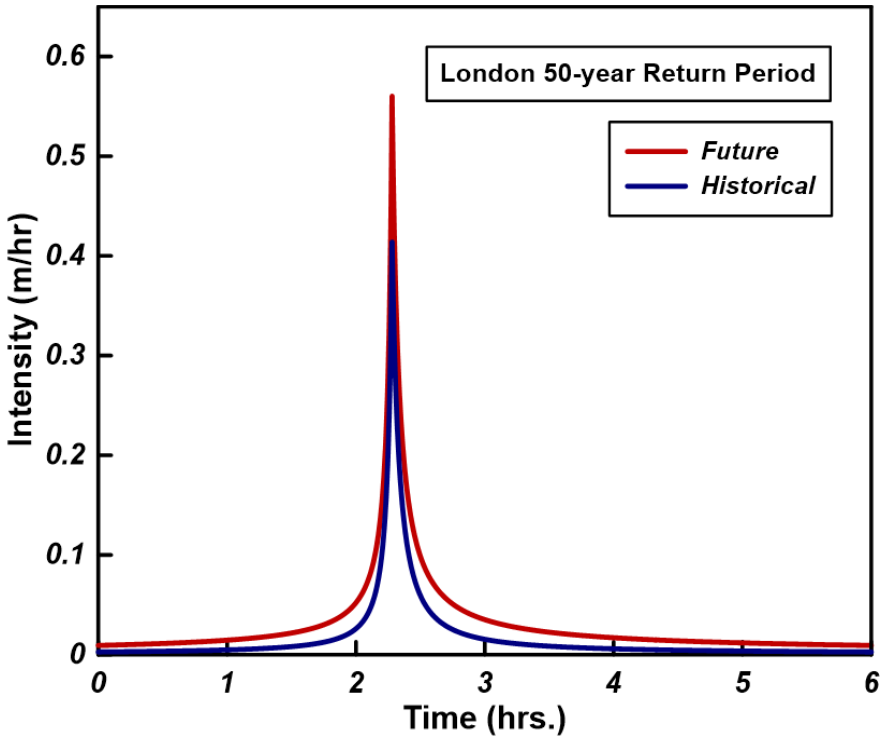
London 50-year Return Period
Future
Historical
Intensity (m/hr)
0.6
0.5
0.4
0.3
0.2
0.1
0
0
1
2
3
4
5
6
Time (hrs.)

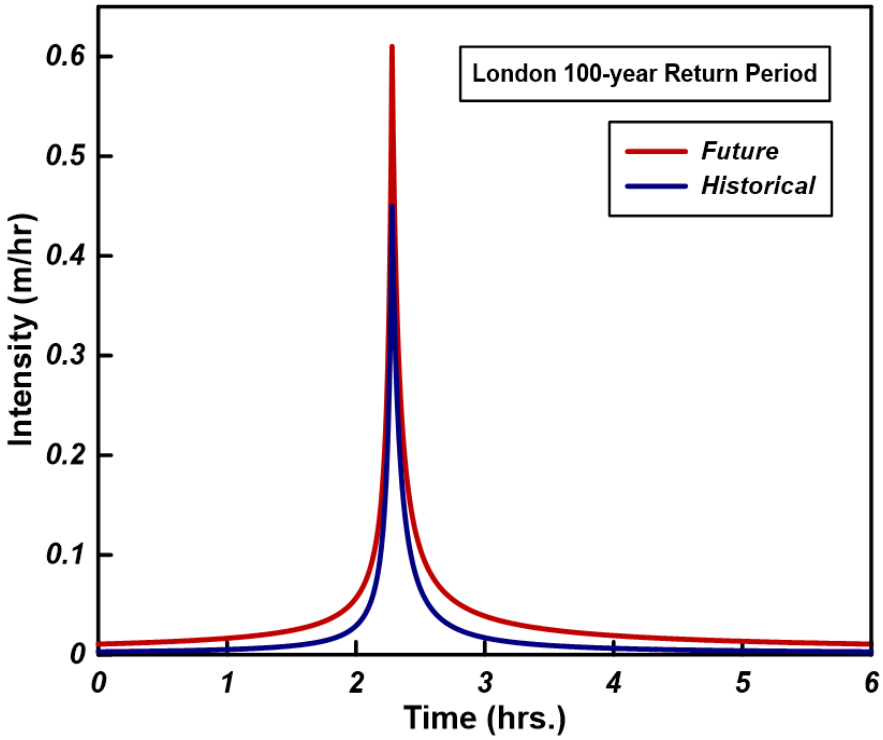
London 100-year Return Period
Future
Historical
Intensity (m/hr)
0.6
0.5
0.4
0.3
0.2
0.1
0
0
1
2
3
4
5
6
Time (hrs.)

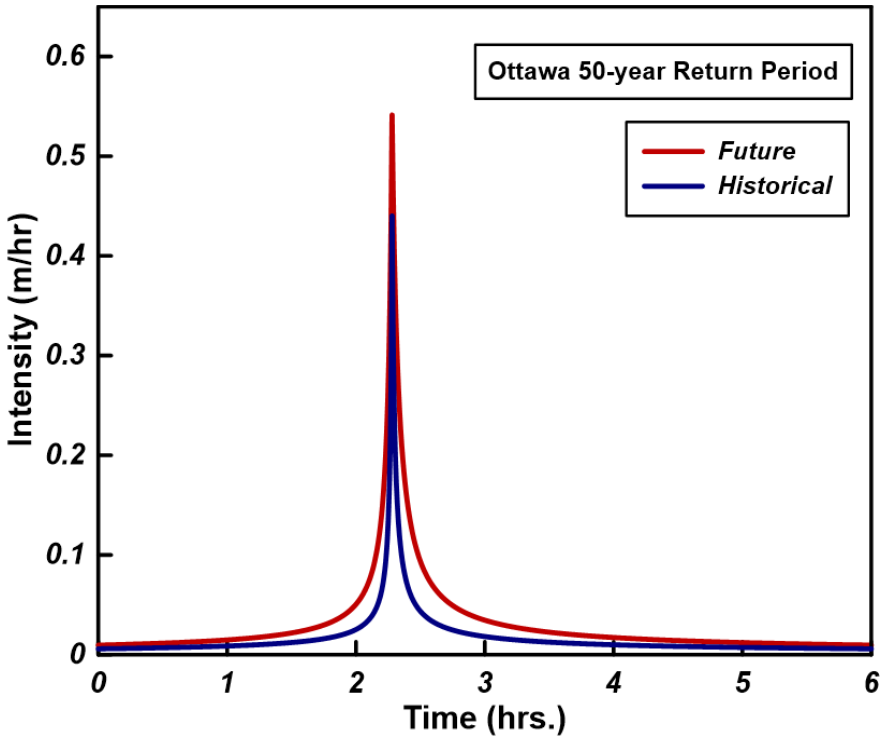
Ottawa 50-year Return Period
Future
Historical
Intensity (m/hr)
0.6
0.5
0.4
0.3
0.2
0.1
0
0
1
2
3
4
5
6
Time (hrs.)

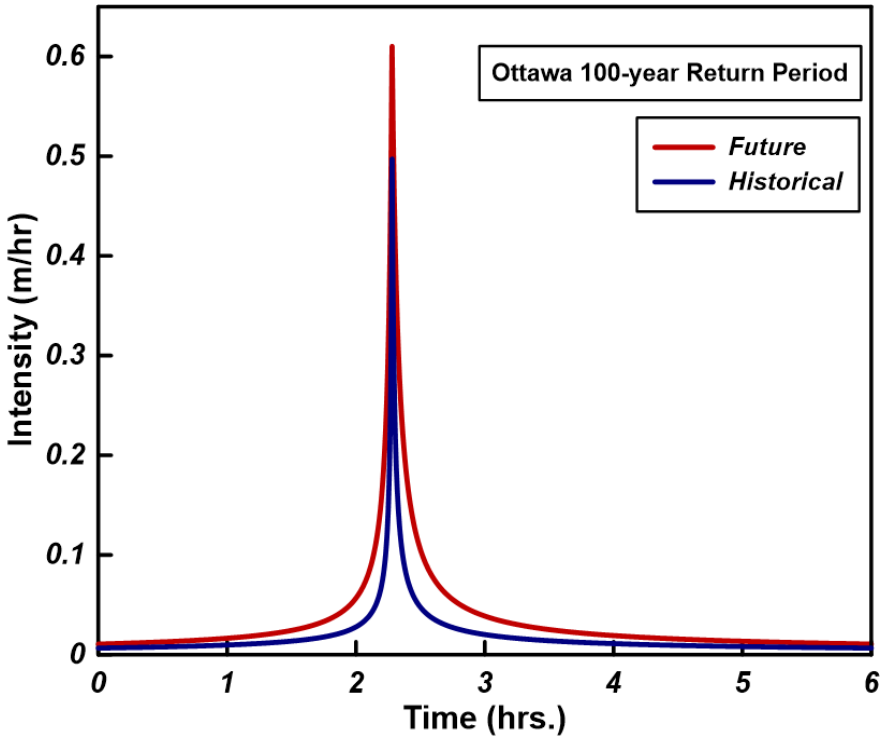
Ottawa 100-year Return Period
Future
Historical
Intensity (m/hr)
0.6
0.5
0.4
0.3
0.2
0.1
0
0
1
2
3
4
5
6
Time (hrs.)

Appendix B: Area of LFS vs Precipitation time and assessment time

Area of LFS <1 (m^2) vs Precipitation time (6 hours) and assessment time (24 hours)

London

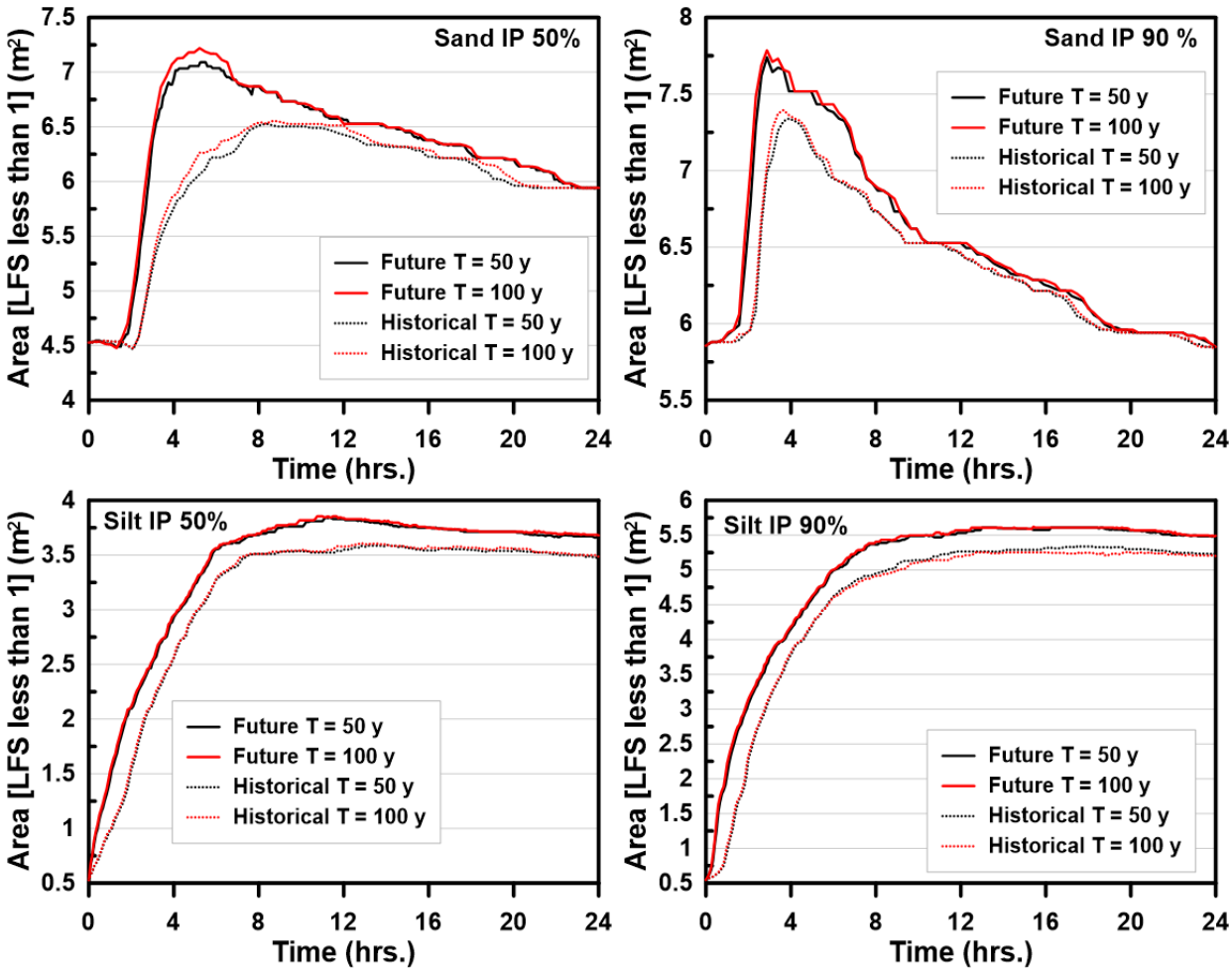

Ottawa

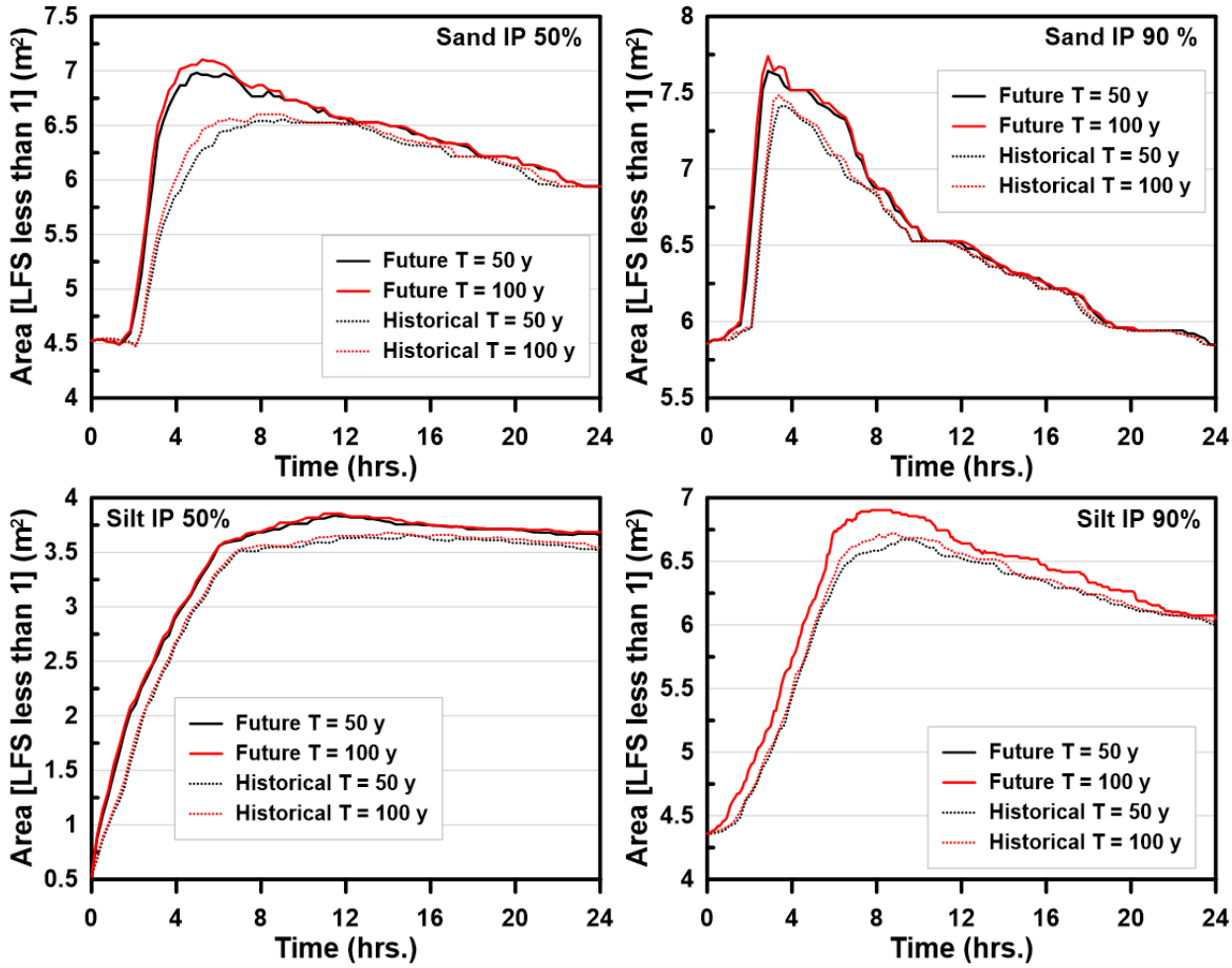
Sand IP 50%
Sand IP 90 %
Silt IP 50%
Silt IP 90%
Area [LFS less than 1] (m²)
Time (hrs.)
Future T = 50 y
Future T = 100 y
Historical T = 50 y
Historical T = 100 y